

We are IntechOpen, the world's leading publisher of Open Access books Built by scientists, for scientists

6,300

Open access books available

171,000

International authors and editors

190M

Downloads

Our authors are among the

154

Countries delivered to

TOP 1%

most cited scientists

12.2%

Contributors from top 500 universities



WEB OF SCIENCE™

Selection of our books indexed in the Book Citation Index
in Web of Science™ Core Collection (BKCI)

Interested in publishing with us?
Contact book.department@intechopen.com

Numbers displayed above are based on latest data collected.
For more information visit www.intechopen.com



Biomaterials and Stem Cells: Promising Tools in Tissue Engineering and Biomedical Applications

Małgorzata Sekuła and Ewa K. Zuba-Surma

Additional information is available at the end of the chapter

<http://dx.doi.org/10.5772/intechopen.70122>

Abstract

Biomaterial sciences and tissue engineering approaches are currently fundamental strategies for the development of regenerative medicine. Stem cells (SCs) are a unique cell type capable of self-renewal and reconstructing damaged tissues. At the present time, adult SCs isolated from postnatal tissues are widely used in clinical applications. Their characteristics such as a multipotent differentiation capacity and immunomodulatory activity make them a promising tool to use in patients. Modern material technologies allow for the development of innovative biomaterials that closely correspond to requirements of the current biomedical application. Biomaterials, such as ceramics and metals, are already used as implants to replace or improve the functionality of the damaged tissue or organ. However, the continuous development of modern technology opens new insights of polymeric and smart material applications. Moreover, biomaterials may enhance the SCs biological activity and their implementation by establishing a specific microenvironment mimicking natural cell niche. Thus, the synergistic advancement in the fields of biomaterial and medical sciences constitutes a challenge for the development of effective therapies in humans including combined applications of novel biomaterials and SCs populations.

Keywords: adult stem cells, biomaterials, regenerative medicine, tissue engineering

1. Introduction

Regenerative medicine represents a new interdisciplinary field of clinical science focused on the development and implementation of novel strategies to enhance the process of regeneration of impaired cells, tissues and organs as well as replacing damaged cells with new, fully functional cells of the required phenotype [1, 2].

To improve the effectiveness of such regeneration processes, one of the potential approaches is application of stem cell (SC)-based therapy. In addition, the combination of stem cells with biocompatible materials that may constitute a scaffold for the seeded cells may lead to enforcement of biological activity of stem cells and as such accelerate the process of regeneration or restoration of impaired tissue [3, 4].

2. Therapeutic applications of stem cells

2.1. Classification and characteristics of stem cells (SCs)

Stem cells (SCs) are a unique type of cells characterized by the ability to (i) self-renewal through unlimited cell divisions and (ii) differentiate into other types of specialized cells, including epithelial, muscle, neuronal cells and others [5, 6].

Based on the origin and source of isolation, SCs may be included in two main groups: (i) embryonic SCs (ESCs)—derived from embryos at different stages of development and (ii) adult SCs (ASCs)—isolated from several postnatal and adult tissue sources, including the umbilical cord, cord blood, bone marrow, adipose tissue, central nervous system, retina, skeletal muscle and other mature tissues [7, 8]. The differentiation capacity of embryonic SCs allows them to form any individual organs and fully differentiated cells of the whole body, which corresponds to pluripotency of these SCs. In opposite, most of adult SCs are multipotent and lineage-restricted (monopotent) and generally give rise to certain cell types of one germ layer or cell lineage. They reside in several niches, including bone marrow, liver, muscle, brain and others, where they may be activate towards tissue- or organ-specific cells under certain physiologic or experimental conditions. Moreover, it has been shown that adult SCs may provide efficient regeneration of impaired organs in both preclinical and clinical conditions [7].

Based on the differentiation capacity, SCs populations belong to the following types [5, 9–11]:

- Totipotent SCs (TSCs)—The most developmentally primitive and potent SCs are capable to differentiate into any cell type from three germ layers (mesoderm, ectoderm and endoderm) forming whole organism as well as into extra-embryonic tissues such as placenta; the best examples of TSCs are zygote and first blastomeres [10–13].
- Pluripotent SCs (PSCs)—The cells sustaining the capacity to differentiate into all cell types from three germ layers, but they are not able to give rise to placenta; PSCs are naturally present in developing embryo in stage of morula, in inner cell mass (ICM) of developing blastocyst and in the epiblast of gastrula and in limited number may also be found in adult tissues as remnants from embryonic development [9, 14]; PSCs may also be de novo created via genetic reprogramming of somatic cells and are called ‘induced PSCs’ (iPS cells) [11, 15].
- Multipotent SCs—The SCs typically capable to give rise to all cell types within one germ layer; the best described examples are mesenchymal SCs (MSCs) isolated from several adult and postnatal tissues [10, 16–18];

- Unipotent SCs (progenitors)—The cells capable to differentiate into one or two particular types of specialized cell present in particular tissue type; this group includes several population of tissue-committed progenitors such as endothelial progenitor cells, cardiac SCs, satellite cells of skeletal muscles, neural progenitors and others [5, 9, 10].

2.2. Types of SCs with potential clinical application

Recently, more attention has been directed to potential utilization of SCs in clinical applications in patients. Due to the legal and ethical restrictions, the employment of embryonic SCs, which possess the largest spectrum of differentiation capacity, is controversial and prohibited in many countries. Moreover, SCs with pluripotent characteristics may lead to adverse side effects following their injection including teratoma formation [19, 20]. Therefore, the therapies employing adult SCs play a major role in human treatment as safe and effective approaches. Transplantations of autologous SCs isolated from mobilized peripheral blood or bone marrow are currently widely used in haematological patients with malignancies such as leukaemia and lymphoma [21]. Moreover, haematopoietic stem cells (HSCs) residing predominantly in adult bone marrow are widely used for bone marrow reconstitution in patients suffering from several genetic and autoimmune diseases, blood cancers and haematopoietic defects [5, 7].

Current growing expectations for further advancements in regenerative medicine are highly focused on mesenchymal stem/stromal cells (MSCs) belonging to adult SCs isolated from several tissue types [16, 18, 22, 23]. MSCs are multipotent, non-haematopoietic cells, which can be isolated from various sources including bone marrow, adipose tissue, cord blood, umbilical cord, Wharton's jelly and other tissues of the adult organism [22, 24]. Isolation of this type of cells does not raise any ethical concerns and is a relatively easy procedure. Moreover, MSCs are characterized by low immunogenicity with simultaneous immunomodulatory effect, and after transplantation, teratoma formation does not occur in the recipient organism [16, 18, 22, 23, 25]. Furthermore, potential regenerative applicability of MSCs is also enhanced by their paracrine activity related to several molecules released to their environment that may impact on other neighbouring cells affecting their functions [22, 25]. MSCs produce and release bioactive molecules, including multitude growth factors (e.g. TGF- β 1, bFGF, BMP-4), anti-inflammatory factors (e.g. IL-10, PGE2, HGF) and cytoprotective agents (e.g. IL-6, MCP-1, IGF-1), which promote resident cells to divide and remodel the damaged tissue [26]. All these listed features make MSCs as promising tool for biomedical research.

MSCs possess a robust proliferation capacity as well as a potential to differentiate into several lineages of mesodermal origin, including bone, cartilage and adipose tissue [23]. Moreover, they have been also shown to give rise to other cell types, such as endothelial, cardiac or liver cells, which may also be utilized in tissue regeneration [16, 27]. These unique biological values may be utilized for the development of personalized treatment strategy for several diseases and provide the progress in establishing modern cell-based therapy. Cell-based therapy represents a promising perspective of treatment directed at the regeneration of damaged tissues or organs using stem cells or progenitor cells both in the autologous and allogeneic system [16, 28–30].

According to the current U.S. National Institutes of Health database including clinical trials conducted worldwide, there are currently more than 240 clinical trials being conducted in the world employing MSCs in patients [31]. Examples of the application of MSCs isolated from different sources in the treatment of selected diseases are shown in **Table 1**.

One of the great new opportunities in medical science is the possibility of obtaining the induced pluripotent SCs (iPS cells) by genetic reprogramming of mature cells into the stage of pluripotency [15]. Due to the discovery of this phenomenon, professor Shinya Yamanaka was honoured with the Nobel Prize in medicine and physiology in 2012. Since then, iPS cells constitute an excellent model for *in vitro* studies of molecular mechanisms associated with the development and progression of several diseases, including Parkinson's disease [32], Huntington disease [33], Down syndrome [34] and others. Moreover, dozens of laboratories are questing for optimal utilization of these cells in tissue regeneration. However, due to the possibility of teratoma formation after iPS transplantation, their applications in medicine are still limited.

Thus, despite the fact that several new rising SCs types are being examined and optimized for future applications, the most commonly applicable SCs in cell therapies of distinct human diseases are adult stem cells including predominantly MSCs derived from bone marrow, adipose tissue and umbilical cord as well as HSCs harvested from bone marrow, mobilized peripheral blood and cord blood [16, 18, 28–30].

Type of MSCs	Condition	ClinicalTrials.gov identifier
Umbilical cord-derived MSCs	Hepatic cirrhosis	NCT02652351
	Aplastic anaemia	NCT03055078
	Stroke	NCT02580019
	Pneumoconiosis	NCT02668068
	Rheumatoid arthritis	NCT02643823
	Sweat gland diseases	NCT02304562
Bone marrow-derived MSCs	Acute myocardial infarction	NCT01652209
	Chronic myocardial ischaemia	NCT02460770
	Acute respiratory distress syndrome	NCT02097641
	Middle cerebral artery infarction	NCT01461720
	Prostate cancer	NCT01983709
	Stroke	NCT02564328
Adipose-derived MSCs	Infantile spinal muscular atrophy	NCT02855112
	Multiple sclerosis	NCT02326935
	Hair restoration	NCT02865421

Source: Ref. [31].

Table 1. The application of MSCs in selected clinical trials.

2.3. Utilization of SC derivatives as a potential alternative to cell-based therapy

Immunomodulatory properties of SCs are important features involved in tissue repair, which are directly related to their paracrine activity. Despite the directly released molecules, mammalian cells, including SCs, are able to produce extracellular vesicles (EVs) carrying bioactive factors, which may additionally be involved in the modulation of the repair process of damaged tissues [35]. EVs represent heterogeneous population of small, circular structures surrounded with the protein-lipid membrane that are released by cells including SCs. Importantly, the size and molecular composition of EVs are different and unique depending on the cell type of origin and the mechanism of their biogenesis. Depending on the size of EVs, they may be distinguished in apoptotic bodies (1–5 μm), microparticles (100 nm–1 μm) and exosomes (30–100 nm) fractions [36, 37].

Several recent scientific reports indicate that EVs express surface markers characterizing the cells from which they are released, along with EV-specific antigens including tetraspanins (CD9, CD63 and CD81), endosome or membrane-binding proteins (TG101), signal transduction or scaffolding proteins (syntenin) [36, 37]. Importantly, EVs may also include various types of bioactive components (e.g. mRNA, miRNA and enzymes), as well as receptors, adhesion or signalling proteins [38, 39]. Importantly, the contents of EVs can be effectively transferred to the target cells, change their function and impact in the regeneration of impaired tissues. Moreover, the presence of protein-lipid membrane on the surface of EVs can protect their bioactive content from extracellular enzymes and therefore the cargo may be delivered in a fully functional form into targeted cells [38, 40]. Thus, EVs are recognized as mediators of intercellular communication and constitute an alternative or reinforcement of a standard cell-based therapy.

The biological relevance of EVs has been established in different experimental settings. Depending on the origin and content of EVs, they may enhance immune system, endorse anti-tumour responses and thus may provide important tools for novel anti-tumour therapies, such as melanoma treatment [41]. EVs may also be utilized as drug delivery vehicles [42], in regenerative medicine [43] and immune therapy [44]. Recently, our study also indicated that SC-derived EVs may be utilized as a novel tool for regenerative therapies of ischemic tissue including in heart repair [38, 40].

However, further studies are required for comprehensive analysis of the mechanisms of EVs action and potential clinical applications of these promising SC derivatives.

3. Medical application of selected natural and synthetic biomaterials

3.1. Material requirements for biomaterials

Biomaterial by definition is a 'substance (other than a drug), synthetic or natural, that can be used as a system or part of a system that treats, augments, or replaces any tissue, organ, or function of the body' [45]. Thus, according to the definition biomaterials are progressively

used in tissue engineering. They may be utilized for the construction of implants to replace lost or damaged organs or tissues and may also constitute a scaffold for enhanced stem cells to reconstruct not fully functional tissue [45, 46].

Due to the wide range of potential applications of biomaterials in regenerative medicine, their physical and chemical properties may be different [45, 47]. However, in order to use a biomaterial in medical application, it should follow relevant requirements such as biocompatibility and biofunctionality [45, 47]:

- Biocompatibility is the ability to integrate with the recipient's cells in a safe manner and without adverse side effects.
- Biofunctionality is the ability to perform a specific biological function, based on the relevant parameters of the physical and mechanical properties.

Other important properties of biomaterials, which are affecting the potential application in medicine, include [45, 48, 49] the following:

- Biodegradation—Decomposition of the material in a natural way, when degradation products remain in the human body but without adverse side effects.
- Bioresorbability—Decomposition of the material in a natural way at a certain period of time after implantation. Non-toxic-degraded products are removed from the body *via* metabolic pathways (hydrolytic or enzymatic degradation).
- Non-toxicity—From the surface or porous of the material does not elute any toxic components, such as surfactants, stabilizers, catalysts, pigments and UV absorbents, which were used during production and that are incompatible with living organisms.
- Mechanical properties—Biomaterial should possess particular mechanical properties consistent with the anatomical site into which it will be implanted.

3.2. Applications of biomaterials

Several biomaterials useful for distinct applications in medical sciences, including in tissue repair and organ reconstruction, have already been developed over the last few decades [45, 47]. The biomaterial sciences are currently one of the highly advancing fields, which also closely cooperate with biotechnological and medical studies. Recent advancement in regenerative medicine strongly requires such strong support from biomaterial sciences, which may provide novel solutions for tissue repair [4, 49].

Among the biomaterials recognized and developed for potential medical purposes, here are multitude materials commonly present in natural sources or *de novo* designed and created for such purposes.

3.2.1. Naturally derived biomaterials

Natural materials commonly present in nature such as agarose, collagen, alginate, chitosan, hyaluronate or fibrin fully cooperate with living tissues of the recipient and possess low

cytotoxicity [47, 48]. Moreover, they may exhibit specific protein-binding sites that improve integration with cells after transplantation [48]. Thus, they are considered predominantly interesting for tissue engineering applications.

One of the most common natural biomaterials is collagen—an important component of connective tissue, including bones, tendons, ligaments and skin [46, 50]. Collagen is simply absorbed into the body, is non-toxic and exhibits a low immune response and as such is a perfect biocompatible material with an adequate mechanical strength and flexibility for several applications. Moreover, collagen enhances cell adhesion to such surface, stimulates also biological interactions between cells and facilitates restoration of the natural microenvironment of cell niche and thereby may support the reconstruction of several damaged tissues [46, 48, 50].

Collagen may be employed for tissue engineering in the form of sponges, gels, hydrogels and sheets. It may also be chemically crosslinked in order to enhance or alter the rate of degradation of the fibres [51]. Currently, collagen preparations are used predominantly in wound healing and cartilage regeneration. Injectable form of collagen is used for cosmetic and aesthetic medicine as a tissue filler. In addition, collagen-based membranes are used in the periodontal treatment as a barrier preventing the migration of epithelial cells. It also forms a favourable microenvironment for stem cells to facilitate reconstruction of the damaged area [50, 51].

3.2.2. Synthetic biomaterials

Synthetic materials are considered as an alternative to natural materials. Due to their defined chemical composition and the ability to control the mechanical and physical properties, they are extensively used in therapeutic applications and basic biological studies [48, 52–55].

Due to distinct variants of polymerization reaction and formation of co-polymers, multiple synthetic polymers with wide range of physical and chemical properties may be achieved in chemical laboratories. Moreover, novel technologies in the synthesis and formation of more complex structures allow for the production of advanced composites [54]. Synthetic polymers, such as poly(ethylene) (PE), polyurethanes (PUR), polylactides (PLA) and poly(glycolide) (PGA), are widely employed as implants and components of medical devices [56]. Moreover, polymers may constitute suitable scaffold for cell propagation and enhance their biological activity, including neural stem cells, retinal progenitor cells or smooth muscle cells [55, 57, 58]. Thus, this group of biomaterials is currently in a special focus of scientists working on combined approaches using biocompatible scaffolds and stem cells for tissue repair [55, 57, 58].

Biodegradable polymers, including polyhydroxycarboxylic acids, such as PGA, PLA, poly(3-hydroxybutyrate), poly(4-hydroxybutyrate) and poly(ϵ -caprolactone) (PCL) are of wide interest in the development of novel technologies [56]. One of their potential applications is utilization in the treatment of cardiovascular diseases. Our recent studies have shown the positive impact of both PCL and PLA scaffolds on proliferation, migration and proangiogenic potential of mesenchymal SCs derived from umbilical cord tissue *in vitro*, suggesting the possible applications of these materials in cardiovascular repair *in vivo* (unpublished data) [59].

Synthetic polymers may also be used in biodegradable stents implanted after a heart attack and greatly contribute to patient recovery [56]. Importantly, the material should have suitable decomposition kinetics. Too long decomposition time (i.e. in the case of PLA or PGA) may lead to late stent thrombosis or blockages [56, 60]. One of a possible solution of this problem is to use rapidly biodegradable polymer stents coated with SCs to help rebuild damaged tissue and additionally stimulate resident cells to grow.

Other types of common synthetic materials useful for biomedical applications are ceramics. It has been well described that ceramic scaffolds, such as, for example, hydroxyapatite (HA) and tri-calcium phosphate (TCP), are characterized by biocompatibility, high mechanical stiffness (Young's modulus), very low elasticity and a hard brittle surface [49]. Due to their chemical and structural similarity to the mineral phase of native bone, these materials may enhance osteoblast proliferation and therefore they are widely utilized in bone regeneration [61, 62]. Moreover, ceramics may be exploited in dental and orthopaedic procedures to fill bone defects or as a bioactive coating material for implants to increase their integration after transplantation [63, 64]. However, their clinical applications are still limited due to the difficulties with the ability to change the shape of the material dedicated for transplantation and controlling time of their degradation rate [49, 65].

Similarly, titanium (Ti)-based metallic materials have been widely optimized for bone repair due to their mechanical properties and resistance to corrosion following the transplantation [66–68]. It has been shown that titanium scaffolds are effectively colonized by osteoblasts responsible for bone formation and this process may be enhanced *via* additional modifications of the scaffold surface by its roughening, coating with HA or graphene oxide (GO), as well as its biofunctionalization with bioactive molecules such as heparin and bone morphogenetic protein 2 (BMP-2) [69–72].

Importantly, graphene in its different forms is currently being considered as a potential new promising material for biomedical applications including tissue repair [73, 74]. This 2D carbon biocompatible material exhibits great electrical, conductive and physical properties, which make it interesting for potential applications for drug delivery and scaffold coating in regenerative therapies [74, 75]. It has been shown that graphene may enhance osteogenic differentiation of SCs [72, 73]. Moreover, our recent data also suggest the beneficial impact of graphene oxide (GO) on proliferative capacity, viability and differentiation potential of umbilical cord tissue-derived MSCs, which confirms the possibility of future graphene employment in tissue repair [76].

3.2.3. Hydrogels

Hydrogels are frequently used biomaterials in the biomedical applications and represent systems consisting of two or more compartments comprising a three-dimensional (3D) network of polymer chains and water that fills the spaces between the macromolecules [77, 78]. The main characteristics of hydrogels include the biocompatibility and ability to swell in solution until they reach a state of equilibrium. These allow them to be injected into the body in a non-invasive manner [77, 78].

Hydrogels demonstrate transparency and bioadhesive properties and they are widely used in the pharmaceutical and dermatological industries by local administration or filling the defects caused by injury [77]. They may also be utilized as an injectable material for bone and cartilage tissue engineering, which may be combined with appropriate cell injection [53, 78, 79]. It has been shown that *in situ* implementation of hydrogels promotes osteoblast differentiation [53, 79]. Therefore, injectable therapy constitutes a promising approach for non-invasive technique of transplantation, where also cell-based component may be added to enhance tissue repair.

3.2.4. Smart materials

Smart materials represent a new generation of biomaterials, exceeding the functionality of the currently widely used construction materials. Smart materials are characterized by the ability to alter their physical characteristics in a controlled manner including changing the shape, colour, stiffness or stickiness in response to several external stimuli, such as temperature, hydrostatic pressure, electric and magnetic field or radiation [80]. These changes are related to the revealing or eliciting the new functionality of the material and may be utilized in biomedical applications. Through the common connection between the internal sensor, the activator and a specific control mechanism, smart materials are able to respond to external stimuli. Importantly, these mechanisms are also responsible for the return to the original state, when a stimulant disappeared [80, 81].

Smart materials include several types such as listed below [52, 80, 82–84]:

- **Colour changing materials**—Materials that change colour in a reversible manner, depending on electrical, optical or thermal changes. These types of materials are exploited, for example, in optoelectronic components, lenses, lithium batteries, ferroelectric memory, temperature sensors or as the indicators of battery consumption [80, 81].
- **Light-emitting materials**—Materials emitting visible or invisible light, as a result of external stimuli such as short wavelength radiation (e.g. X-rays, ultraviolet light), temperature and electric voltage. They are utilized in electronics, filters for glasses, devices that detect UV rays, in criminology and in geology to identify minerals and rocks. They may also be exploited as a component of protective clothing, safety elements and warning materials [80, 81].
- **Shape memory materials**—Metal alloys that change shape as a result of temperature increase or decrease, respectively, to the set value. The reversibility of the process is to return to its original shape by changing the temperature or under the influence of the applied motion (the effect of pseudoelasticity). These materials are used in temperature sensors, electronics, robotics, telecommunications and production of medical devices (micro-pump, surgical clamps, orthodontic wire, long- and short-term implants, suture tightening on a stiffen wound, orthopaedic devices, bone nails, clamps, surgical instruments and others) [83, 84].
- **Self-assembling materials**—Materials that exhibit the intrinsic ability to spontaneously connect individual elements into an ordered 2D or 3D structure. In addition, they can also

have the ability to bind metal atoms, ions, molecules or semiconductors. They are widely used in biological research and nanotechnology, that is, in the tissue regeneration, as components for the storage of drugs, crystal engineering, as artificial proteins with pH-sensitive structure, as semi-permeable membrane as well as for the production of electronic processors and displays [52, 82].

- **Self-repairing materials**—Structural damage of this type of material is automatically and autonomously recovered by inducing a change in the shape or the self-assembly of the molecules. This process is not a method of complete repair of the impaired material; however, it may be used in the military, automotive, aviation and electronics industries [52, 82].

4. Novel aspects of the application of stem cells and biomaterials in tissue engineering and regenerative medicine

4.1. Biomaterials approaches for enhancement of SCs-based therapy

Modern approaches in current regenerative medicine include developing biocompatible scaffolds and combining them with living cell of selected type and bioactive molecules, in order to enhance the regeneration process of damaged tissues and organs [47].

Growing evidence indicate different populations of stem cells as a promising tool that may be utilized in tissue engineering and repair. Importantly, despite the regenerative properties of SCs, the restoration processes in damaged tissue are long and may not often be fully effective for functional recovery of damaged tissue. On the other hand, appropriate stimulation of reparative capacity of SCs may be achieved by modulation of chemical and physical properties of optimized biomaterials [47, 70, 77]. Therefore, simultaneous application of optimized and well-combined SCs and biomaterials may open new perspectives for the synergistic effective cooperation of both such components to improve the efficiency of the regeneration process [77]. Biomaterials may enhance the biological activity of SCs by establishing a specific niche related to their native microenvironment. This type of cell-biomaterial interactions leads to stimulation of cell adhesion, proliferation and directed differentiation of the cells implemented at the injured site [47, 70, 77]. Therefore, therapy based on biomaterials and SCs opens new possibilities for the development of innovative medicine [47, 77].

Currently, growing evidence is focused on encapsulation of native SCs prior to their transplantation [47, 85]. Cells encapsulation technique is based on the immobilization of cells in a semi-permeable membrane, which protects cells against mechanical damage and immune system response. Notably, the construction of the microcapsules allows bidirectional diffusion of nutrients, oxygen and wastes and therefore provides appropriate conditions for cell development [47, 85].

Encapsulated cells may be subjected to transplantation and directed differentiation. The material used to construct the microcapsules should possess particular physical properties,

such as biocompatibility, mechanical stability, permeability, appropriate size, strength and durability [47]. One of the most common encapsulation materials is alginate. Due to the fact that the procedure for cell encapsulation using alginate can be performed under physiological conditions (physiological temperature and pH) and using isotonic solutions, it is widely distributed through clinical and industrial applications. Moreover, this natural biodegradable polymer that mimics the extracellular matrix and promotes cell functions and metabolism has been established in cartilage regenerative approaches [86, 87]. Microencapsulation technology represents a novel cell culture system that allows maintaining cell viability and differentiation of interested cell lines. It also may support the extracellular matrix production and cell organization in reconstructed tissue [86].

5. Conclusions

Significant advancement of regenerative medicine, nanomedicine and biomaterials engineering offers extended possibilities to obtain novel, effective achievements, which may be utilized in biomedical applications. The effect of interdisciplinary activity resulted in the development of bioactive scaffolds that promote cell propagation and enhance their biological activity. However, some difficulties in biomaterial- and cell-based therapy are still unclear and need to be addressed for widespread investigations. Nevertheless, integrative research in biomaterials and medicine fields is a challenge to develop effective therapies for cancer, civilization diseases and provide further development of tissue engineering.

Acknowledgements

This work is supported by grants from the National Science Centre (NCN): SONATA BIS-3 (UMO-2013/10/E/NZ3/007500), SYMFONIA 3 (UMO-2015/16/W/NZ4/00071) and the National Centre for Research and Development (NCBR): STRATEGMED III (BioMiStem project; ID 303570) to EZS. The Faculty of Biochemistry, Biophysics and Biotechnology at the Jagiellonian University, Krakow, Poland, is a partner of the Leading National Research Center (KNOW) supported by the Ministry of Science and Higher Education.

Author details

Małgorzata Sekuła¹ and Ewa K. Zuba-Surma^{2*}

*Address all correspondence to: ewa.zuba-surma@uj.edu.pl

1 Malopolska Centre of Biotechnology, Jagiellonian University, Krakow, Poland

2 Department of Cell Biology, Faculty of Biochemistry, Biophysics and Biotechnology, Jagiellonian University, Krakow, Poland

References

- [1] Galliot B, Crescenzi M, Jacinto A, Tajbakhsh S. Trends in tissue repair and regeneration. *Development*. 2017;**144**:357-364. DOI: 10.1242/dev.144279
- [2] Forbes SJ, Rosenthal N. Preparing the ground for tissue regeneration: From mechanism to therapy. *Nature Medicine*. 2014;**20**:857-869. DOI: 10.1038/nm.3653
- [3] Sahito RG, Sureshkumar P, Sotiriadou I, Srinivasan SP, Sabour D, Hescheler J, et al. The potential application of biomaterials in cardiac stem cell therapy. *Current Medicinal Chemistry*. 2016;**23**:589-602. DOI: 10.2174/092986732306160303151041
- [4] Shafiq M, Jung Y, Kim SH. Insight on stem cell preconditioning and instructive biomaterials to enhance cell adhesion, retention, and engraftment for tissue repair. *Biomaterials*. 2016;**90**:85-115. DOI: 10.1016/j.biomaterials.2016.03.020
- [5] Hima Bindu A, Srilatha B. Potency of various types of stem cells and their transplantation. *Journal of Stem Cell Research & Therapy*. 2011;**1**:1-6. DOI: 10.4172/2157-7633.1000115
- [6] Ghodsizad A, Voelkel T, Moebius J, Gregoric I, Bordel V, Straach E, et al. Biological similarities between mesenchymal stem cells (MSCs) and fibroblasts. *Journal of Cytology & Histology*. 2010;**1**:1-6. DOI: 10.4172/2157-7099.1000101
- [7] Novik AA, Kuznetsov A, Melnichenko VY, Fedorenko DA, Ionova TI, Gorodokin GV. Non-myeloablative autologous haematopoietic stem cell transplantation with consolidation therapy using mitoxantrone as a treatment option in multiple sclerosis patients. *Stem Cell Research & Therapy*. 2011;**1**:1-5. DOI: 10.4172/2157-7633.1000102
- [8] Toma JG, Akhavan M, Fernandes KJ, Barnabé-Heider F, Sadikot A, Kaplan DR, et al. Isolation of multipotent adult stem cells from the dermis of mammalian skin. *Nature Cell Biology*. 2001;**3**:778-784. DOI: 10.1038/ncb0901-778
- [9] Ratajczak MZ, Ratajczak J, Suszynska M, Miller DM, Kucia M, Shin DM. A novel view of the adult stem cell compartment from the perspective of a quiescent population of very small embryonic-like stem cells. *Circulation Research*. 2017;**120**:166-178. DOI: 10.1161/CIRCRESAHA.116.309362
- [10] Daley GQ. Stem cells and the evolving notion of cellular identity. *Philosophical Transactions of the Royal Society of London Series B, Biological Sciences*. 2015;**370**:20140376. DOI: 10.1098/rstb.2014.0376
- [11] Cahan P, Daley GQ. Origins and implications of pluripotent stem cell variability and heterogeneity. *Nature Reviews Molecular Cell Biology*. 2013;**14**:357-368. DOI: 10.1038/nrm3584
- [12] Thomson JA, Itskovitz-Eldor J, Shapiro SS, Waknitz MA, Swiergiel JJ, Marshall VS, et al. Embryonic stem cell lines derived from human blastocysts. *Science*. 1998;**282**:1145-1147. DOI: 10.1126/science.282.5391.1145

- [13] Suwinska A, Czolowska R, Ozdzanski W, Tarkowski AK. Blastomeres of the mouse embryo lose totipotency after the fifth cleavage division: Expression of Cdx2 and Oct4 and developmental potential of inner and outer blastomeres of 16- and 32-cell embryos. *Developmental Biology*. 2008;**322**:133-144. DOI: 10.1016/j.ydbio.2008.07.019
- [14] Kucia M, Reza R, Campbell FR, Zuba-Surma E, Majka M, Ratajczak J, et al. A population of very small embryonic-like (VSEL) CXCR4(+)SSEA-1(+)Oct-4+ stem cells identified in adult bone marrow. *Leukemia*. 2006;**20**:857-869. DOI: 10.1038/sj.leu.2404171
- [15] Takahashi K, Yamanaka S. Induction of pluripotent stem cells from mouse embryonic and adult fibroblast cultures by defined factors. *Cell*. 2006;**126**:663-676. DOI: 10.1016/j.cell.2006.07.024
- [16] Chugh AR, Zuba-Surma EK, Dawn B. Bone marrow-derived mesenchymal stem cells and cardiac repair. *Minerva Cardioangiologica*. 2009;**57**:185-202
- [17] Kobolak J, Dinnyes A, Memic A, Khademhosseini A, Mobasher A. Mesenchymal stem cells: Identification, phenotypic characterization, biological properties and potential for regenerative medicine through biomaterial micro-engineering of their niche. *Methods*. 2016;**99**:62-68. DOI: 10.1016/j.ymeth.2015.09.016
- [18] Malek A, Bersinger NA. Human placental stem cells: Biomedical potential and clinical relevance. *Journal of Stem Cells*. 2011;**6**:75-92
- [19] Kamada M, Mitsui Y, Matsuo T, Takahashi T. Reversible transformation and de-differentiation of human cells derived from induced pluripotent stem cell teratomas. *Human Cell*. 2016;**29**:1-9. DOI: 10.1007/s13577-015-0119-1
- [20] Masuda S, Yokoo T, Sugimoto N, Doi M, Fujishiro SH, Takeuchi K, et al. A simplified in vitro teratoma assay for pluripotent stem cells injected into rodent fetal organs. *Cell Medicine*. 2012;**3**:103-112. DOI: 10.3727/215517912X639351
- [21] Wang B, Ren C, Zhang W, Ma X, Xia B, Sheng Z. Intensified therapy followed by autologous stem-cell transplantation (ASCT) versus conventional therapy as first-line treatment of follicular lymphoma: A meta-analysis. *Journal of Hematology & Oncology*. 2013;**31**:29-33. DOI: 10.1002/hon.2015
- [22] Hass R, Kasper C, Böhm S, Jacobs R. Different populations and sources of human mesenchymal stem cells (MSC): A comparison of adult and neonatal tissue-derived MSC. *Cell Communication and Signaling*. 2011;**9**:1-59. DOI: 10.1186/1478-811X-9-12
- [23] Jin HJ, Bae YK, Kim M, Kwon SJ, Jeon HB, Choi SJ, et al. Comparative analysis of human mesenchymal stem cells from bone marrow, adipose tissue, and umbilical cord blood as sources of cell therapy. *International Journal of Molecular Sciences*. 2013;**14**:17986-18001. DOI: 10.3390/ijms140917986
- [24] Wei X, Yang X, Han ZP, Qu FF, Shao L, Shi YF. Mesenchymal stem cells: A new trend for cell therapy. *Acta Pharmacologica Sinica*. 2013;**34**:747-754. DOI: 10.1038/aps.2013.50

- [25] Gnecci M, Zhang Z, Ni A, Dzau VJ. Paracrine mechanisms in adult stem cell signaling and therapy. *Circulation Research*. 2008;**103**:1204-1219. DOI: 10.1161/CIRCRESAHA.108.176826
- [26] Mirotsov M, Jayawardena TM, Schmeckpeper J, Gnecci M, Dzau VJ. Paracrine mechanisms of stem cell reparative and regenerative actions in the heart. *Journal of Molecular and Cellular Cardiology*. 2011;**50**:280-289. DOI: 10.1016/j.yjmcc.2010.08.005
- [27] Labeledz-Maslowska A, Lipert B, Berdecka D, Kedracka-Krok S, Jankowska U, Kamycka E, et al. Monocyte chemoattractant protein-induced protein 1 (MCP1) enhances angiogenic and cardiomyogenic potential of murine bone marrow-derived mesenchymal stem cells. *PloS One*. 2015;**10**:e0133746. DOI: 10.1371/journal.pone.0133746
- [28] Mobashera A, Kalamegame G, Musumecif G, Batt ME. Chondrocyte and mesenchymal stem cell-based therapies for cartilage repair in osteoarthritis and related orthopaedic conditions. *Maturitas*. 2014;**78**:188-198. DOI: 10.1016/j.maturitas.2014.04.017
- [29] Samanta A, Kaja AK, Afzal MR, Zuba-Surma EK, Dawn B. Bone marrow cells for heart repair: Clinical evidence and perspectives. *Minerva Cardioangiologica*. 2017;**65**:299-313
- [30] Afzal MR, Samanta A, Shah ZI, Jeevanantham V, Abdel-Latif A, Zuba-Surma EK, et al. Adult bone marrow cell therapy for ischemic heart disease: Evidence and insights from randomized controlled trials. *Circulation Research*. 2015;**117**:558-575. DOI: 10.1161/CIRCRESAHA.114.304792
- [31] Health AsotUNIo. 2017. Available from: <https://clinicaltrials.gov/> [cited: 18 February 2017]
- [32] Byers B, Lee HL, Reijo Pera R. Modeling Parkinson's disease using induced pluripotent stem cells. *Current Neurology and Neuroscience Reports*. 2012;**12**:237-242. DOI: 10.1007/s11910-012-0270-y
- [33] Tousley A, Kegel-Gleason KB. Induced pluripotent stem cells in Huntington's disease research: Progress and opportunity. *Journal of Huntington's Disease*. 2016;**5**:99-131. DOI: 10.3233/JHD-160199
- [34] Brigida AL, Siniscalco D. Induced pluripotent stem cells as a cellular model for studying Down syndrome. *Journal of Stem Cells & Regenerative Medicine*. 2012;**12**:54-60
- [35] Yanez-Mo M, Siljander PR, Andreu Z, Zavec AB, Borrás FE, Buzas EI, et al. Biological properties of extracellular vesicles and their physiological functions. *Journal of Extracellular Vesicles*. 2015;**4**:1-60. DOI: 10.3402/jev.v4.27066
- [36] György B, Szabó TG, Pásztói M, Pál Z, Misják P, Aradi B, et al. Membrane vesicles, current state-of-the-art: Emerging role of extracellular vesicles. *Cellular and Molecular Life Sciences*. 2011;**68**:2667-2688. DOI: 10.1007/s00018-011-0689-3
- [37] Lötvall J, Hill AF, Hochberg F, Buzás EI, Di Vizio D, Gardiner C, et al. Minimal experimental requirements for definition of extracellular vesicles and their functions: A position statement from the International Society for Extracellular Vesicles. *Journal of Extracellular Vesicles*. 2014;**3**:1-21. DOI: 10.3402/jev.v3.26913

- [38] Bobis-Wozowicz S, Kmiotek K, Sekula M, Kedracka-Krok S, Kamycka E, Adamiak M, et al. Human induced pluripotent stem cell-derived microvesicles transmit RNAs and proteins to recipient mature heart cells modulating cell fate and behavior. *Stem Cells*. 2015;**33**:2748-2761. DOI: 10.1002/stem.2078
- [39] Camussi G, Deregibus MC, Bruno S, Grange C, Fonsato V, Tetta C. Exosome/microvesicle-mediated epigenetic reprogramming of cells. *American Journal of Cancer Research*. 2011;**1**:98-110
- [40] Bobis-Wozowicz S, Kmiotek K, Kania K, Karnas E, Labedz-Maslowska A, Sekula M, et al. Diverse impact of xeno-free conditions on biological and regenerative properties of hUC-MSCs and their extracellular vesicles. *Journal of Molecular Medicine*. 2017;**95**:205-220. DOI: 10.1007/s00109-016-1471-7
- [41] Escudier B, Dorval T, Chaput N, André F, Caby M, Novault S, et al. Vaccination of metastatic melanoma patients with autologous dendritic cell (DC) derived-exosomes: Results of the first phase I clinical trial. *Journal of Translational Medicine*. 2005;**3**:1-13. DOI: 10.1186/1479-5876-3-10
- [42] Pascucci L, Coccè V, Bonomi A, Ami D, Ceccarelli P, Ciusani E, et al. Paclitaxel is incorporated by mesenchymal stromal cells and released in exosomes that inhibit in vitro tumor growth: A new approach for drug delivery. *Journal of Controlled Release*. 2014;**192**:262-270. DOI: 10.1016/j.jconrel.2014.07.042
- [43] Xin H, Li Y, Liu Z, Wang X, Shang X, Cui Y, et al. MiR-133b promotes neural plasticity and functional recovery after treatment of stroke with multipotent mesenchymal stromal cells in rats via transfer of exosome-enriched extracellular particles. *Stem Cells*. 2016;**31**:2733-2746. DOI: 10.1002/stem.1409
- [44] Kordelas L, Rebmann V, Ludwig A, Radtke S, Ruesing J, Doeppner T, et al. MSC-derived exosomes: A novel tool to treat therapy-refractory graft-versus-host disease. *Leukemia*. 2014;**28**:970-973. DOI: 10.1038/leu.2014.41
- [45] Williams DF. *The Williams Dictionary of Biomaterials*. Liverpool University Press. 1999. ISBN: 0853237344
- [46] Jiang J, Papoutsakis ET. Stem-cell niche based comparative analysis of chemical and nano-mechanical material properties impacting ex vivo expansion and differentiation of hematopoietic and mesenchymal stem cells. *Advanced Healthcare Materials*. 2013;**2**:25-42. DOI: 10.1002/adhm.201200169
- [47] Perán M, García MA, López-Ruiz E, Bustamante M, Jiménez G, Madeddu R, et al. Functionalized nanostructures with application in regenerative medicine. *International Journal of Molecular Sciences*. 2012;**13**:3847-3886. DOI: 10.3390/ijms13033847
- [48] Reis R, Cohn D. *Polymer Based Systems on Tissue Engineering, Replacement and Regeneration*. Springer Science & Business Media; Nato Science Series II 2002. DOI: 10.1007/978-94-010-0305-6. ISBN: 9781402010002
- [49] O'Brien F. Biomaterials & scaffolds for tissue engineering. *Materials Today*. 2011;**14**:88-95. DOI: 10.1016/S1369-7021(11)70058-X

- [50] Khan R, Khan MH. Use of collagen as a biomaterial: An update. *Journal of Indian Society of Periodontology*. 2013;**17**:539-542. DOI: 10.4103/0972-124X.118333
- [51] Patino MG, Neiders ME, Andreana S, Noble B, Cohen RE. Collagen as an implantable material in medicine and dentistry. *Journal of Oral Implantology*. 2002;**28**:220-225. DOI: 10.1563/AAID-JOI-D-13-00063
- [52] Chen JK, Chang CJ. Fabrications and applications of stimulus-responsive polymer films and patterns on surfaces: A review. *Materials*. 2014;**7**:805-875. DOI: 10.3390/ma7020805
- [53] Kondiah PJ, Choonara YE, Kondiah PPD, Marimuthu T, Kumar P, du Toit LC, et al. A review of injectable polymeric hydrogel systems for application in bone tissue engineering. *Molecules*. 2016;**21**:1-31. DOI: 10.3390/molecules21111580
- [54] Maitz M. Applications of synthetic polymers in clinical medicine. *Biosurface and Biotribology*. 2015;**1**:161-176. DOI: 10.1016/j.bsbt.2015.08.002
- [55] Tomita M, Lavik E, Klassen H, Zahir T, Langer R, Young MJ. Biodegradable polymer composite grafts promote the survival and differentiation of retinal progenitor cells. *Stem Cells*. 2005;**23**:1579-1588. DOI: 10.1634/stemcells.2005-0111
- [56] Strohbach A, Busch R. Polymers for cardiovascular stent coatings. *International Journal of Polymer Science*. 2015;**2015**:1-11. DOI:10.1155/2015/782653
- [57] Bhang S, Lim J, Choi C, Kwon Y, Kim B. The behavior of neural stem cells on biodegradable synthetic polymers. *Journal of Biomaterials Science, Polymer Edition*. 2007;**18**:223-239. DOI: 10.1163/156856207779116711
- [58] Yim EK, Reano RM, Pang SW, Yee AF, Chen CS, Leong KW. Nanopattern-induced changes in morphology and motility of smooth muscle cells. *Biomaterials*. 2005;**26**:5405-5413. DOI: 10.1016/j.biomaterials.2005.01.058
- [59] Sekula M, Domalik-Pyzik P, Morawska-ChochóŁ A, Czuchnowski J, Madeja Z, Zuba-Surma E, et al., editors. Utilization of biocompatible and biodegradable polymers in stem cell research and biomedical applications. In: 27th European Conference on Biomaterials (ESB 2015); Krakow, Poland; 2015
- [60] Sengel CT. Delivery of nanoparticles for the treatment of cardiovascular diseases. *Global Journal of Obesity, Diabetes and Metabolic Syndrome*. 2015;**2**:18-21. DOI: 10.17352/2455-8583.000010
- [61] Ambrosio AM, Sahota JS, Khan Y, Laurencin CT. A novel amorphous calcium phosphate polymer ceramic for bone repair: I. Synthesis and characterization. *Journal of Biomedical Materials Research*. 2001;**58**:295-301. DOI: 10.1002/1097-4636(2001)58:3<295::AID-JBM1020>3.0.CO;2-8
- [62] Smith IO, McCabe LR, Baumann MJ. MC3T3-E1 osteoblast attachment and proliferation on porous hydroxyapatite scaffolds fabricated with nanophase powder. *International Journal of Nanomedicine*. 2006;**1**:189-194. DOI: 10.2147/nano.2006.1.2.189

- [63] Al-Sanabani J, Madfa A, Al-Sanabani F. Application of calcium phosphate materials in dentistry. *International Journal of Biomaterials*. 2013;**2013**:1-12. DOI: 10.1155/2013/876132
- [64] McEntirea BJ, Bala BS, Rahamanc MN, Chevalierd J, Pezzottie G. Ceramics and ceramic coatings in orthopaedics. *Journal of the European Ceramic Society*. 2015;**23**:4327-4369. DOI: 10.1016/j.jeurceramsoc.2015.07.034
- [65] Wang M. Developing bioactive composite materials for tissue replacement. *Biomaterials*. 2003;**24**:2133-2151. DOI: 10.1016/S0142-9612(03)00037-1
- [66] Nair M, Elizabeth E. Applications of titania nanotubes in bone biology. *Journal of Nanoscience and Nanotechnology*. 2015;**15**:939-955. DOI: 10.1166/jnn.2015.9771
- [67] Vanderleyden E, Mullens S, Luyten J, Dubruel P. Implantable (bio)polymer coated titanium scaffolds: A review. *Current Pharmaceutical Design*. 2012;**18**:2576-2590. DOI: 10.2174/138161212800492903
- [68] Oliveira NT, Guastaldi AC. Electrochemical stability and corrosion resistance of Ti-Mo alloys for biomedical applications. *Acta Biomaterialia*. 2009;**5**:399-405. DOI: 10.1016/j.actbio.2008.07.010
- [69] Gao Y, Zou S, Liu X, Bao C, Hu J. The effect of surface immobilized bisphosphonates on the fixation of hydroxyapatite-coated titanium implants in ovariectomized rats. *Biomaterials*. 2009;**30**:1790-1796. DOI: 10.1016/j.biomaterials.2008.12.025
- [70] Elias CN, Oshida Y, Lima JH, Muller CA. Relationship between surface properties (roughness, wettability and morphology) of titanium and dental implant removal torque. *Journal of the Mechanical Behavior of Biomedical Materials*. 2008;**1**:234-242. DOI: 10.1016/j.jmbbm.2007.12.002
- [71] Kim SE, Song SH, Yun YP, Choi BJ, Kwon IK, Bae MS, et al. The effect of immobilization of heparin and bone morphogenic protein-2 (BMP-2) to titanium surfaces on inflammation and osteoblast function. *Biomaterials*. 2011;**32**:366-373. DOI: 10.1016/j.biomaterials.2010.09.008
- [72] Zancanela DC, Simao AM, Francisco CG, de Faria AN, Ramos AP, Goncalves RR, et al. Graphene oxide and titanium: Synergistic effects on the biomineralization ability of osteoblast cultures. *Journal of Materials Science: Materials in Medicine*. 2016;**27**:71. DOI: 10.1007/s10856-016-5680-y
- [73] Xie C, Sun H, Wang K, Zheng W, Lu X, Ren F. Graphene oxide nanolayers as nanoparticle anchors on biomaterial surfaces with nanostructures and charge balance for bone regeneration. *Journal of Biomedical Materials Research Part A*. 2017;**5**:1311-1323. DOI: 10.1002/jbm.a.36010
- [74] Kumar S, Chatterjee K. Comprehensive review on the use of graphene-based substrates for regenerative medicine and biomedical devices. *ACS Applied Materials & Interfaces*. 2016;**8**:26431-26457. DOI: 10.1021/acsami.6b09801

- [75] Bikhof Torbati M, Ebrahimian M, Yousefi M, Shaabanzadeh M. GO-PEG as a drug nano-carrier and its antiproliferative effect on human cervical cancer cell line. *Artificial Cells, Nanomedicine, and Biotechnology*. 2017;**45**:568-573. DOI: 10.3109/21691401.2016.1161641
- [76] Liu Y, Chen T, Du F, Gu M, Zhang P, Zhang X, et al. Single-layer graphene enhances the osteogenic differentiation of human mesenchymal stem cells in vitro and in vivo. *Journal of Biomedical Nanotechnology*. 2016;**12**:1270-1284. DOI: 10.1166/jbn.2016.2254
- [77] Assunção-Silva RC, Gomes ED, Sousa N, Silva NA, Salgado AJ. Hydrogels and cell based therapies in spinal cord injury regeneration. *Stem Cells International*. 2015;**2015**:1-24. DOI: 10.1155/2015/948040
- [78] Wang T, Lai JH, Yang F. Effects of hydrogel stiffness and extracellular compositions on modulating cartilage regeneration by mixed populations of stem cells and chondrocytes in vivo. *Tissue Engineering Part A*. 2016;**22**:1348-1356. DOI: 10.1089/ten.TEA.2016.0306
- [79] Niranjana R, Koushik C, Saravanan S, Moorthi A, Vairamani M, Selvamurugan N. A novel injectable temperature-sensitive zinc doped chitosan/ β -glycerophosphate hydrogel for bone tissue engineering. *International Journal of Biological Macromolecules*. 2013;**54**:24-29. DOI: 10.1016/j.ijbiomac.2012.11.026
- [80] Susmita K. Introduction, classification and applications of smart materials: An overview. *American Journal of Applied Sciences*. 2013;**10**:876-880. DOI: 10.3844/ajassp.2013.876.880
- [81] Wang ZL, Kang ZC. *Functional and Smart Materials Structural Evolution and Structure Analysis*. Plenum Press New York; 1998. DOI: 10.1007/978-1-4615-5367-0. ISBN-13: 978-1-4613-7449-7
- [82] Bekas DG, Tsirka K, Baltzis D, Paipetis AS. Self-healing materials: A review of advances in materials, evaluation, characterization and monitoring techniques. *Composites Part B: Engineering*. 2016;**87**:92-119. DOI: 10.1016/j.compositesb.2015.09.057
- [83] El Feninat F, Laroche G, Fiset M, Mantovani D. Shape memory materials for biomedical applications. *Advanced Engineering Materials*. 2002;**4**:91-104. DOI:10.1002/1527-2648(200203)4:3<91::AID-ADEM91>3.0.CO;2-B
- [84] Chan BQY, Kenny Low ZW, Jun Wen Heng S, Chan SY, Owh C, Jun Loh X. Recent advances in shape memory soft materials for biomedical applications. *Applied Materials & Interfaces*. 2016;**8**:10070-10087. DOI: 10.1021/acsami.6b01295
- [85] Murua A, Portero A, Orive G, Hernández RM, de Castro M, Pedraz JL. Cell microencapsulation technology: Towards clinical application. *Journal of Controlled Release*. 2008;**132**:76-83. DOI: 10.1016/j.jconrel.2008.08.010
- [86] Ghidoni I, Chlapanidas T, Bucco M, Crovato F, Marazzi M, Vigo D, et al. Alginate cell encapsulation: New advances in reproduction and cartilage regenerative medicine. *Cytotechnology*. 2008;**58**:49-56. DOI: 10.1007/s10616-008-9161-0
- [87] Hunt NC, Grover LM. Cell encapsulation using biopolymer gels for regenerative medicine. *Biotechnology Letters*. 2010;**32**:733-742. DOI: 10.1007/s10529-010-0221-0

We are IntechOpen, the world's leading publisher of Open Access books Built by scientists, for scientists

6,300

Open access books available

171,000

International authors and editors

190M

Downloads

Our authors are among the

154

Countries delivered to

TOP 1%

most cited scientists

12.2%

Contributors from top 500 universities



WEB OF SCIENCE™

Selection of our books indexed in the Book Citation Index
in Web of Science™ Core Collection (BKCI)

Interested in publishing with us?
Contact book.department@intechopen.com

Numbers displayed above are based on latest data collected.
For more information visit www.intechopen.com



Identification of Fe₃O₄ Nanoparticles Biomedical Purpose by Magnetometric Methods

Zoia Duriagina, Roman Holyaka, Tetiana Tepla,
Volodymyr Kulyk, Peter Arras and Elena Eynorn

Additional information is available at the end of the chapter

<http://dx.doi.org/10.5772/intechopen.69717>

Abstract

The application of magnetic nanoparticles for biomedical research is an interdisciplinary problem. The use of nano- and microsized powder materials as developed technology for obtaining bionanomaterials with magnetocatalytic properties has been investigated. Control over immobilization can be carried by means of magnetic properties. Synthesis of superparamagnetic nanoparticles is developed not only for the benefit of fundamental science, but also for many technologies, such as technologies of magnetic storage media, magnetic ink for printers, but mainly for biosensors and medical applications. All the biomedical applications require that the nanoparticles have high enough levels of saturation of magnetization; their size should be less than 100 nm with a small deviation in size. Appropriate coating of the surface of magnetic nanoparticles should be nontoxic, biocompatible with the target of bioorganic compound. The techniques of measurement of magnetic nanoparticle properties by means of vibrational magnetometers, as well as by means of a set of smart sensor devices in accordance with new concept of Internet of Things (IoTh), were described. The first method is based on vibrating sample magnetometer technique. The second method is based on direct measurement of three dimensions (3D) of nanoparticles' magnetic field components.

Keywords: magnetic nanoparticles, drug transportation, magnetic field sensor

1. Introduction

Use of nanomaterials has become one of the innovation research directions in materials science, biochemistry and medicine. Small sizes of nanoparticles (NPs) lead to the appearance

of new unique functional properties. The methods of such material preparation are improving every year and become more accessible. The technology of material structure “design” by combining different types of materials, starting from metals, their compounds (oxides, nitrides, borides and hydrides) and ending with organic and inorganic polymers [1], has recently been widely used. Nanomaterials based on metals operate in power generating, optical industry and biomedicine. The unique superparamagnetic, optical and electrochemical properties are accentuated first of all. Use of magnetic nanoparticles (MNPs) for biomedical researches is an interdisciplinary problem and to solve it experts in different areas are required—medical workers, biologists, specialists in the field of materials science and electrodynamics. Application of nanomaterials with coating for biomedical purposes foresees such functional properties of the given system as adsorption, adhesion strength, biocompatibility, and certain magnetic and optoelectronic properties that will identify the stability of the obtained structure-energy state. The task of the materials science researchers is to develop complicated nanoobjects with optimal properties and morphological structure and to create the system of monitoring (Internet of Things (IoTh)) by their life activity cycle. The perfect biomedical systems can be considered such that the stable functional properties are possessed.

In particular, magnetism of nanoparticles is an important information carrier and what is especially valuable can be implemented through industrial means. This action at a distance in combination with a typical magnetic field penetration into human body tissues opens many new applications, including transport and purposeful delivery of biomagnets to a corresponding biological object [2]. Magnetism can be exhibited in a greater number of new nanomaterials. It is known that, under transition to nanosizes in metals and their compounds, new specific characteristics appear. Thus, magnetic properties of bulk gold and platinum are nonmagnetic, but at the nanosize they are magnetic. Surface atoms are not only different to bulk atoms, but they can also be modified by interaction with other chemical species, that is, by capping the nanoparticles. This phenomenon opens the possibility to modify the physical properties of the nanoparticles by capping them with appropriate molecules. Actually, it should be possible that nonferromagnetic bulk materials exhibit ferromagnetic-like behavior when prepared in a nanorange. One can obtain magnetic nanoparticles of Pd, Pt and the surprising case of Au (that is diamagnetic in bulk) from nonmagnetic bulk materials. In the case of Pt and Pd we can obtain the ferromagnetism. However, gold nanoparticles become ferromagnetic when they are capped with appropriate molecules: the charge localized at the particle surface gives rise to ferromagnetic-like behavior. This observation suggested that modification of the d band structure by chemical bonding can induce ferromagnetic-like character in metallic clusters [3].

2. Use of magnetic nanoparticles in medicine

Magnetic biomaterials are widely used in medicine, especially in cardiology, neurosurgery, oncology, radiology and cellular biology for cell separation, to perform immunological analysis, magnetic resonance spectroscopy, information preservation and so on [1–8]. They are also used as the X-ray contrast means and magnetosensitive composites for drugs and genes delivery, in radionuclide therapy and hyperthermia (**Figure 1**). Such applications are

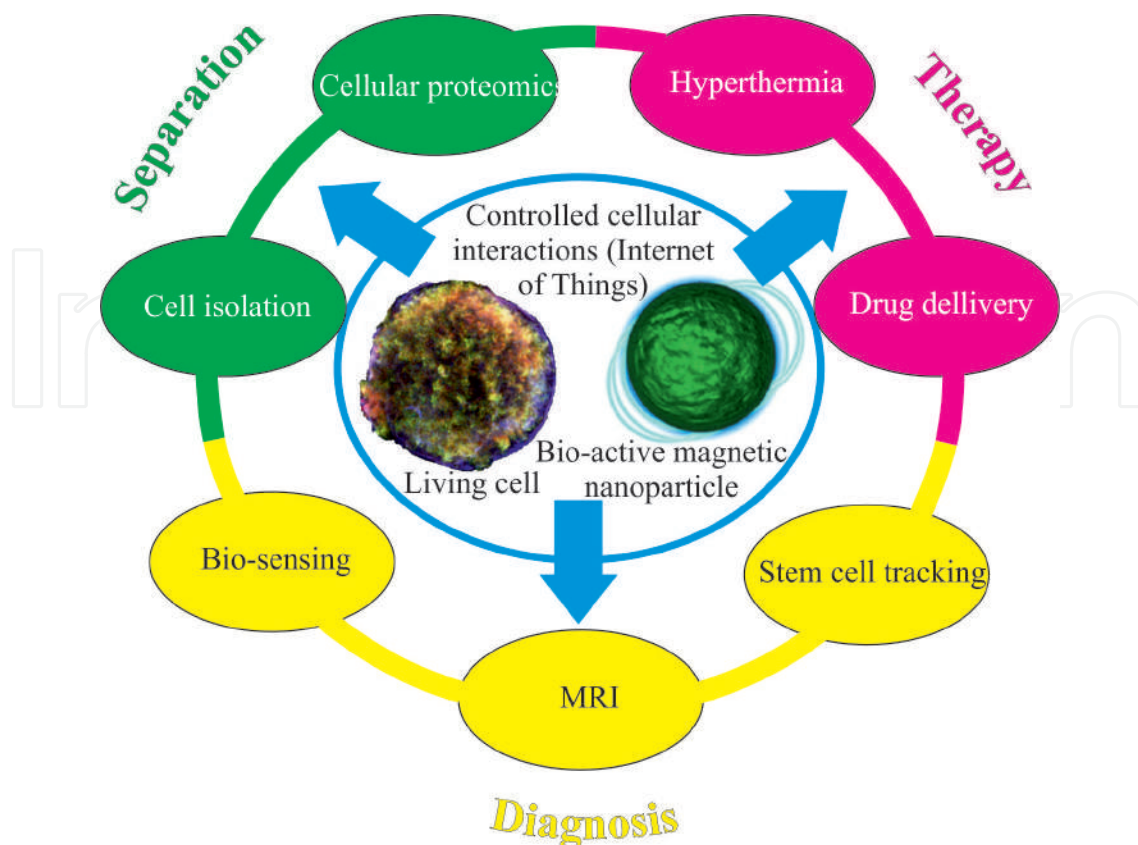


Figure 1. Use of magnetic nanoparticles in medicine.

perspective in case the clearly defined and checked interaction between magnetic nanoparticles and living cells is provided.

It is known that living organisms are built of cells with usual sizes of about 10 μm . The objects from which a cell consists of are much less than 1 μm . It should be considered that the synthesized nanoparticles are of sizes 2–450 nm, commensurable with the sizes of intercellular biological objects, viruses, proteins and genes. Thus, the nanoparticles by the sizes and mass occupy the intermediate place between single molecule and living cells. Still the main advantage of these materials is their ability to perform the preset functions under the effect of external magnetic field (**Figure 2**).

This occurs due to the formation of potential barriers at their boundary that limit the charge carrier movement in different directions and give the electron processes a mainly quantum character with dominating role of the interface. It should be noted that in this case a non-linear dependence of equilibrium concentration of defects at the interface is observed that increases the dependence of properties on nanostructure sizes [10]. This is especially important when delivering drugs and means of diagnostics. Depending on the sizes, other properties of nanoparticles as toxicity, adsorption ability and magnetism also change. In particular, when the size of nanoparticles is less than 10 nm, they pass into a superparamagnetic state that, when adsorbing the energy of the external high-frequency electromagnetic field, promotes conversion of the energy state into the thermal one. This enables a tumor heating to a temperature of 43°C and thus its destruction [11, 12].

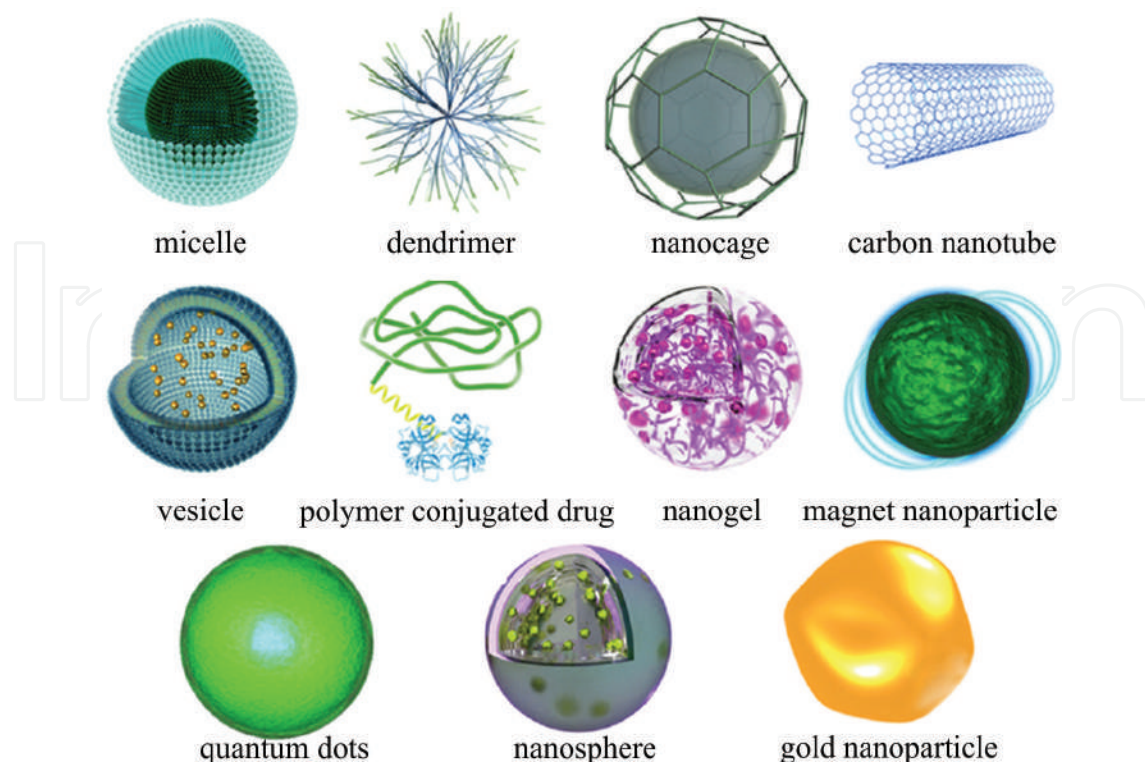


Figure 2. Several classes of NP used for the design of smart micro/nanocarriers, including micelles, dendrimers, nanocages, CNT, polymeric conjugates, nanogels, magnetic NP, quantum dots (QD), nanospheres and gold (Au) NP [9].

It has recently been proven that the effects of heat are more cytotoxic for cancer cells than they are for surrounding normal cells. Because of this, researchers have focused on hyperthermia as a method to selectively treat cancer cells. In Gilchrist's invaluable study, the cancer cells were heated locally using magnetic NP with a 1.2-MHz magnetic field. Since then, other observations have demonstrated that magnetic-induced hyperthermia in animals that have been injected directly with MNP can produce tumor regression through the application of magnetic fields to the solid tumors [9].

For therapeutic aims, magnetic nanoparticles are rarely used in a pure form. Usually, they are encapsulated or situated in bioinert matrices made of different organic compounds (**Figure 3**). This allows decreasing of the possible toxic effect of magnetic phase and simultaneous increasing of its stability due to immobilization on the surface of such capsules or matrices of medical aids. Encapsulation is usually carried out in suspensions of ultradispersive ferromagnetic or superparamagnetic particles containing stabilizing reagents—so called magnetic liquids [2, 5].

The structure of a multifunctional/multimodality MNP with a magnetic core, a polymeric coating and targeting ligands extended from the surface of MNP with the aid of polymeric spacers. Therapeutic payloads (drugs and genes) and imaging reporters (fluorophores and radionuclides) can be either embedded in the coating, or conjugated on the surface [5].

Magnetic contrast agents using which an image of a human body is obtained with a nuclear magnetic resonance tomography are widely known. Particles of these agents consist of a core

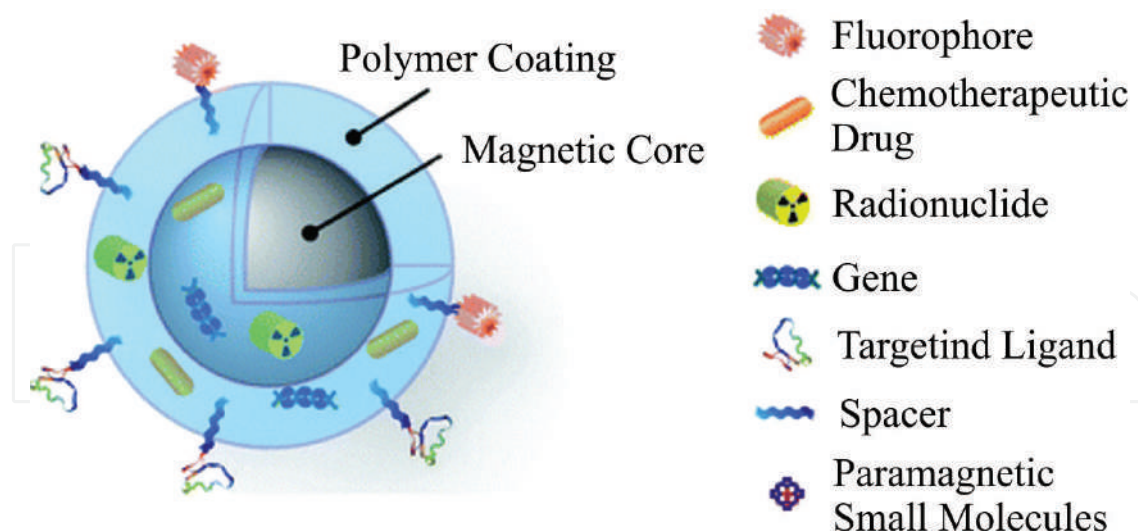


Figure 3. Graphic illustration of the structure of a multifunctional/multimodality MNP and different types of magnetic cores.

form magnetite or maghemite and a shell from dextran or silicon. Colloid solutions based on biomolecule-sorbed magnetic iron oxides, surrounded by a polymer layer, can be used for interaction with biological targets and direct them into a tumor with the aim of treatment or diagnostics. In this case, the controlled movement of magnetic particles in a body occurs because of the use of magnetic field gradient, regulated such that particles penetrate directly into the affected area [4].

Magnetic nanoparticle-based drugs can be divided into two groups: for external use (ointments, applicators, etc.) and for internal use (liquids, suspensions and magnetic containers). To improve physicochemical and medical biological properties when delivering drugs, the sizes of magnetic material particles in the blood stream should not exceed 100 nm. Under such conditions, they can be also used for hypoferritic anemia treatment. Today, the drugs obtained by adding precious metals to iron are paid more and more attention to. They are used as anti-inflammatory, antibacterial, anticancer and anesthetic compounds of the ointments for external use.

Magnetic carriers of medical purpose should be biocompatible with a human organism, non-toxic and nonallergenic. To improve biocompatibility, magnetic carriers are coated with chitosan, dextran, starch, carbon, gelatin, polymer starch coatings and so on (**Figure 4**). It should be noted that silicon oxide also increases biocompatibility of nanoparticles, and in this case, iron is localized inside the SiO₂ particles as in microcapsule. Release rate of drugs in these conditions can be regulated by changing the size and porosity of the obtained systems [4].

Recently, nano- and microsize powder materials are based on Fe₃O₄, especially in combination with bioselective elements—ferments have been widely used. This is important for developing technologies of manufacturing bionanomaterials with catalytic properties. High chemical activity of Fe₃O₄ particles is caused by their higher ability to ion or atomic exchange, adsorption and formation of surface ligaments with other adsorbed particles. This guarantees

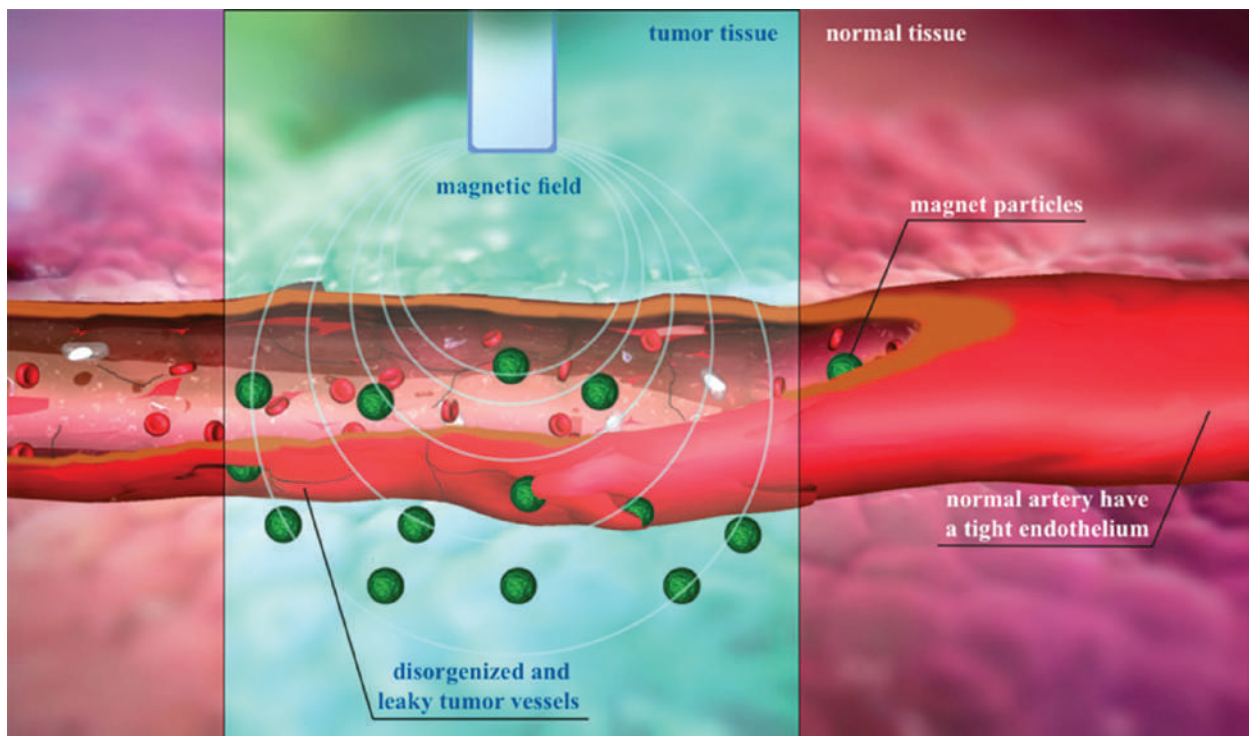


Figure 4. Schematic representation of the proposed magnetic sensitive carrier and triggered drug release mechanism [9].

the creation of bioparticles (immobilized ferments on the particle surface) with their further use in biosensorics and in enzymatic reactions. It is known that powder particles of Fe_3O_4 retain magnetization even if no external magnetic field is present, possessing own magnetic moment. However, remaining magnetization has a negative effect—a tendency of nanoparticles to agglomeration. Therefore, for the effective use of such magnetic particles, their chemical stability should be ensured by applying the corresponding coating on their surface.

2.1. Methods of obtaining magnetic nanoparticles

Physical and chemical properties of magnetic nanoparticles are determined by their structure and method of preparation. In most cases, these are particles of size from 1 to 100 nm with clearly expressed superparamagnetism. The most widely used methods of magnetic nanoparticle synthesis are as follows:

- Deposition—synthesis of iron oxides from water solutions of their salts in inert gas atmosphere at ambient or elevated temperature.
- Thermal decomposition—synthesis of Fe_3O_4 nanoparticles during decomposition of organic metal compounds in boiling organic solvents that contain stabilizing surface active agents (SAA).
- Microemulsion technology.

To synthesize magnetite-based nanocomposites, the following methodical approaches are mainly used [13–16].

- Precipitation in the conditions of oxidizing hydrolysis of iron sulfate Fe²⁺ in acid environment.
- Precipitation in the conditions of alkali hydrolysis of iron chlorides Fe²⁺ and Fe³⁺.
- Precipitate deposition from the solutions of iron chlorides Fe²⁺ and Fe³⁺ under alkali hydrolysis of urea.

When modifying the conditions of magnetite core synthesis and forming the core shell, it is possible to obtain magnetic nanocomposites that differ not only by size but also by the ratio of “core–shell” sizes, magnetic susceptibility and complexity of surface microrelief that will specify the absorption properties.

However, nanoparticle synthesis has remained until now a complicated task. This is related with the difficulty of formation of homodispersive population of checked-size magnetic particles. It should be noted that there is no still a complete understanding of the mechanisms of core formation and growth. Besides the technology of obtaining crystalline nanoparticles with high saturation, magnetization needs further improvement. Moreover, nanoparticles lose their stability with time. This occurs due to the decrease of their free surface energy as a result of agglomeration. It is necessary to develop strategies of the surface coating preparation to simplify the process and effectively prevent agglomeration and segmentation of superparamagnetic particles. As a result, a stable solution for injections or frozen-dried (lyophilized) powder, that is easily dissolved, can be obtained [17].

Investigation of superparamagnetic nanoparticles, especially Fe₃O₄ nanoparticles, should be aimed at establishing the interrelations between their structure and pharmacokinetics. Nature of the coating on the iron oxide surface will determine not only the size of colloids but also will affect the pharmacokinetics and metabolic properties. This will enable modeling of their capture by reticuloendothelial system (RES) and facilitate diffusion to the tumor tissue. Processes of modification of magnetic nanoparticle surface, which are used for connection of biovectors, must be also improved. This is decisive in optimization of superparamagnetic nanoparticles likeness with biological objects [18].

2.2. Properties of Fe₃O₄ magnetite

Iron oxides (in particular magnetite) are among the most investigated materials in human history. Synthesis of superparamagnetic nanoparticles of iron oxide Fe₃O₄ is developing for the sake of fundamental science and technological applications, as for example magnetic data carriers, for biosensor, medical applications and magnetic inks [19–21]. Superparamagnetic nanoparticles of iron oxide with corresponding surface microgeometry can be used for increasing the image contrast, restoration of tissues, detoxification of biological fluids, hyperthermia, directed delivery of drugs and cell separation.

Detailed characterization of magnetite NPs is therefore necessary in order to obtain an accurate relationship between their electronic, magnetic and structural properties. Nominally claimed magnetite NPs are often (and to various extents) composed of nonstoichiometric oxide phases, and their instability in air ultimately causes oxidation to maghemite. The oxidization rate of

magnetite NPs in ambient conditions is size-dependent and can range from several months for NPs <10 nm, up to several years for NPs ~100 nm. However, there is no general consensus regarding the complex oxidation mechanism, which presumably proceeds through a continual set of intermediate phases accompanied by cations and vacancies (C–V) reordering. Magnetite and maghemite both crystallize in the face-centered cubic (fcc) spinel structure, whose unit cell is composed of 32 O^{2-} ions placed at the 32e crystallographic position, and 24 Fe ions distributed over the 64 tetrahedral 8a (A) and 32 octahedral 16d (B) crystallographic positions (**Figure 5**). Magnetite and maghemite can be represented with a single formula: $(Fe^{3+})_A[(Fe^{2+})_{1-3\delta}(Fe^{3+})_{1+2\delta}]_B O^4$, where δ stands for vacancies and $0 \leq \delta \leq 1/3$. In pure magnetite ($\delta = 0$), all A sites are occupied by Fe^{3+} ions, while B sites are equally occupied with Fe^{2+} and Fe^{3+} . In pure maghemite ($\delta = 1/3$), all Fe ions are in 3+ state, with a tendency to regular arrangement

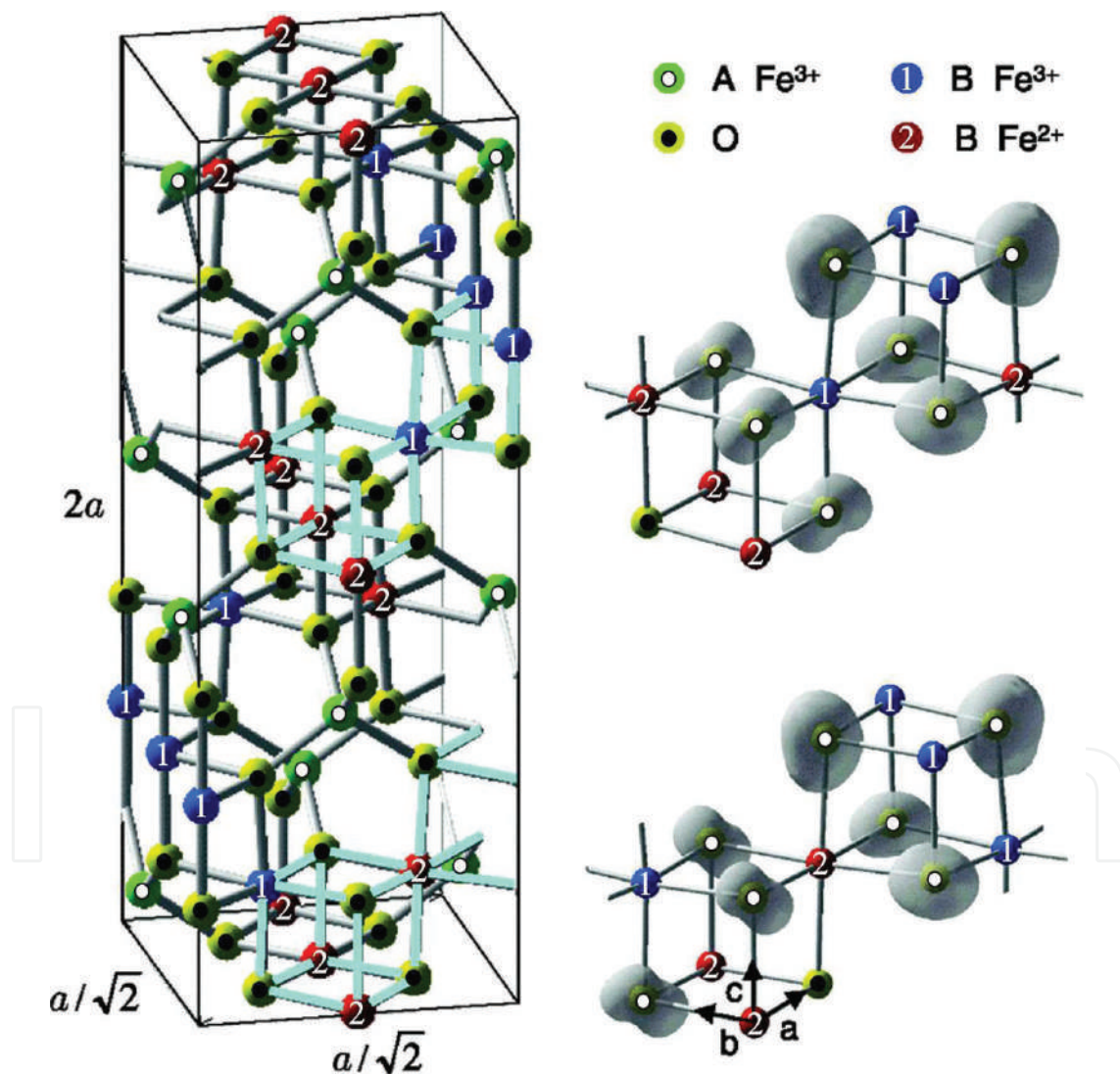


Figure 5. Left: monoclinic crystal structure of Fe_3O_4 in the low-temperature phase corresponding to a subcell of $a_2 \times a_2 \times 2a$ with $P2_1/c$ symmetry. Right: 3D isosurfaces of unoccupied density of states of the O 2p integrated between the fermi level and 1 eV above within the corresponding Fe_3O_4 cubes highlighted in the crystal structure. For simplicity, we denote the octahedral Fe site with nominal 2+ and 3+ valences as Fe^{2+} and Fe^{3+} , respectively [22].

at B sites (two occupied followed by one vacant site). Vacancies occur preferentially at octahedral sites, but they can also mix over octahedral and tetrahedral sites. The degree of vacancy ordering in maghemite decreases with a particle size, and it is believed that for NPs smaller than 20 nm vacancy ordering vanishes. Magnetite and maghemite are both ferrimagnetic (the two uneven ferromagnetic sublattices Fe_A and Fe_B are antiferromagnetically aligned), with comparable saturation magnetizations (MS = 90 emu/g for magnetite; MS = 83.5 emu/g for well-ordered crystalline maghemite samples) and extraordinary high Curie temperatures (TC = 858 K magnetite; TC = 790–893 K maghemite, depending on the degree of C–V ordering).

The important difference between magnetite and maghemite is that maghemite is an insulator with energy gap $E_g \approx 2$ eV, while magnetite is half-metal with much narrower $E_g = 0.1$ –0.5 eV (depending on the sample quality). Furthermore, bulk magnetite undergoes so-called Verwey order-disorder phase transition to the insulating state at temperatures 120–125 K, accompanied with structural change from cubic to monoclinic lattice symmetry and various anomalies in the physical properties. The decisive influence on this complex transformation is ascribed to charge and orbital ordering involved in the three-site distortions. The exact structural parameters of the low temperature (LT) crystal structure, which is thought to have at least four inequivalent octahedral Fe sites, are extremely difficult to determine.

Things are even more elusive when the sample size is in the nanometer range. According to some recent reports for NPs with the mean size ~ 50 nm, the Verwey temperature (TV) shifts down to 20 K and it cannot be observed for smaller particles. The Verwey transition is weakly size-dependent in magnetite NPs larger than 20 nm, slightly suppressed in NPs smaller than 20 nm, and completely vanishes for NPs smaller than 6 nm. These inconsistencies are often ascribed to the fact that final properties of magnetite NPs strongly depend also on structural order [23].

2.3. Investigation of the structure and properties of Fe₃O₄ nanoparticles

In this research, the Fe₃O₄-NP characterization was performed by infrared Fourier spectroscopy using spectrophotometer Bruker Vertex 70 with attachment attenuated total reflectance (ATR). Powder samples were dried on the microscope slide surface and irradiated by a laser beam.

The intensive peak from Fe₃O₄-NP at 600 cm⁻¹, similarly to micro X-ray spectral analysis, indicated the presence of Fe–O bonds in Fe₃O₄-NP (**Figure 6, Table 1**). Peak intensity increases from the value of 1200 cm⁻¹, and in the range of 600–1200 cm⁻¹ a significant background of the wave number area of the substances of glass on which the samples were dried is observed. In this range, only a signal from Si–O (for a wave number 1053 cm⁻¹) is clearly seen. The blind area should contain signals from C–O (for a wave number of about 1100 cm⁻¹) and signals of group Si–O–C (for a wave number of about 1108 cm⁻¹).

Obtained data can be used as an introductory information for processing monitoring of dynamics in situ of nanoparticle modification.

Size of Fe₃O₄ particles strongly affects its microstructure and properties. **Figure 7** presents a difference in microstructure of Fe₃O₄ micro- and nanoparticles.

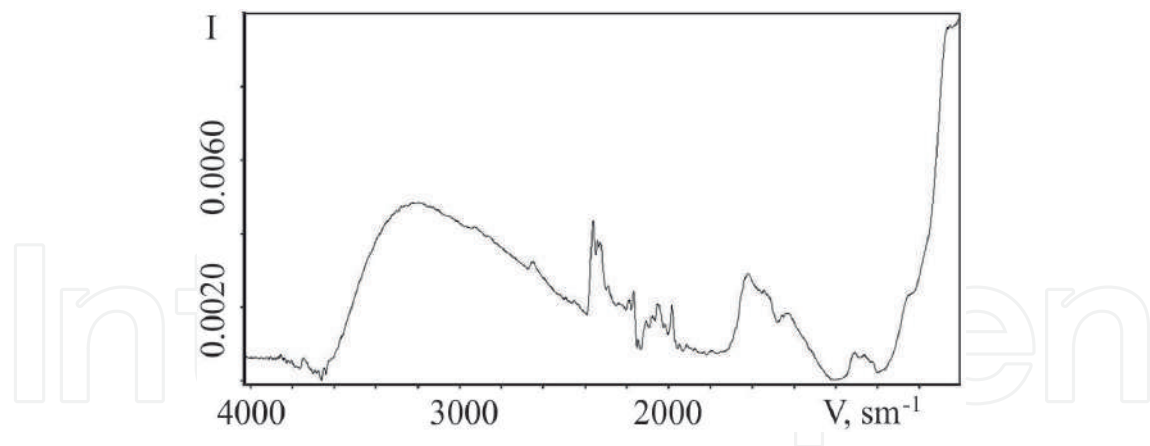


Figure 6. IR-Fourier spectra of Fe_3O_4 nanoparticles.

To estimate the sizes of Fe_3O_4 -NP atomic-force microscopy was used, which software products allowed the establishment of the scanned particle structure (**Figure 8**). Investigation data prove the results of microscopic investigations on the spherical nanoparticle accumulation. Two types of structural inhomogeneity can be distinguished on the investigated sample surface: conglomerates of conical-like nanoparticles and granular texture of substrate. Surface topography is characterized by a rough relief with morphological regions of blocked structure. Blocks are characterized by nonisometric round form with no surface faceting. Their height above the substrate surface is in the range from 5 to 10 nm and base diameter from 30 to 50 nm. In this case, the dominant size of nanoparticles is 8 nm.

It is established at the same time that the size of Fe_3O_4 microparticles is about $1\mu\text{m}$ (**Figure 9(b)**).

Use of Fe_3O_4 nanoparticles with the aim of their functionalization (application of shells, medical aids and markers on them) or introduction in a living organism for hyperthermia foresees the application of surface coating. In this case, the analysis of the dimensions and properties of nanoparticles using a simple method becomes more complex [24]. In such cases, magnetic methods become one of the methods of particle categorization.

2.4. Methods of magnetic properties investigation

Among the magnetic research methods in materials science, the magnetic phase analysis is especially widely used. Its possibilities and effectiveness to a great extent are determined

Wave number (cm^{-1})	Chemical bond
3230	-OH valence vibrations
1617	-OH deformation ("wagging")
1421	Not described
600	Fe-O

Table 1. Correspondence of IR-Fourier spectra peaks of Fe_3O_4 -NP to chemical bonds [13–16].

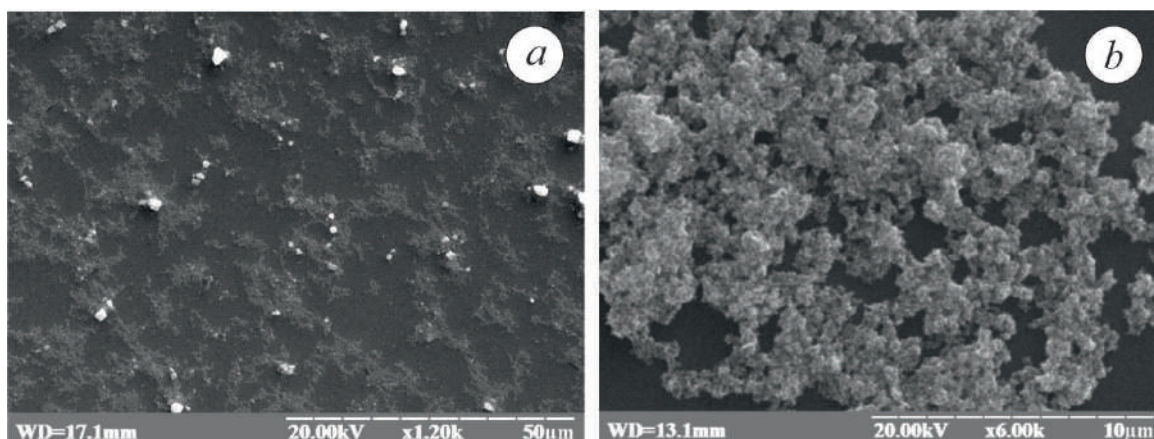


Figure 7. Microstructure of synthesized Fe₃O₄: (a) Fe₃O₄ nanoparticles; (b) Fe₃O₄ microparticles. Microstructures were obtained according to the scanning microscopy data.

by technical characteristics of the equipment. The quantitative phase magnetic analysis uses properties of ferromagnetics, which they acquire in strong magnetic fields—in the state of technical saturation. Primary magnetic properties that are structurally insensitive are obtained from the curve of temperature dependence of saturation magnetization. Such characteristics are magnetization and Curie point. These values give the information about phase composition of material and its changes in the process of certain thermal operations and also in the process of deformation. Curie point and saturation magnetization are called primary magnetic properties because their values are determined by the nature of the ferromagnetic phase (crystal lattice, electron structure of atoms and chemical phase composition) [25].

Changes in magnetization and Curie point of separate phases observed in the process of investigation of a certain material are not caused by their particle growth but are conditioned by the change of chemical composition of phases and their crystalline composition only. Based on these data, it is possible to study the kinetics of phase formation at the very early stages of the process (for particles sizes up to 10⁻⁶ cm) by the growth of magnetization and Curie point to their normal values. Thus, a weak dependence of saturation magnetization and Curie point

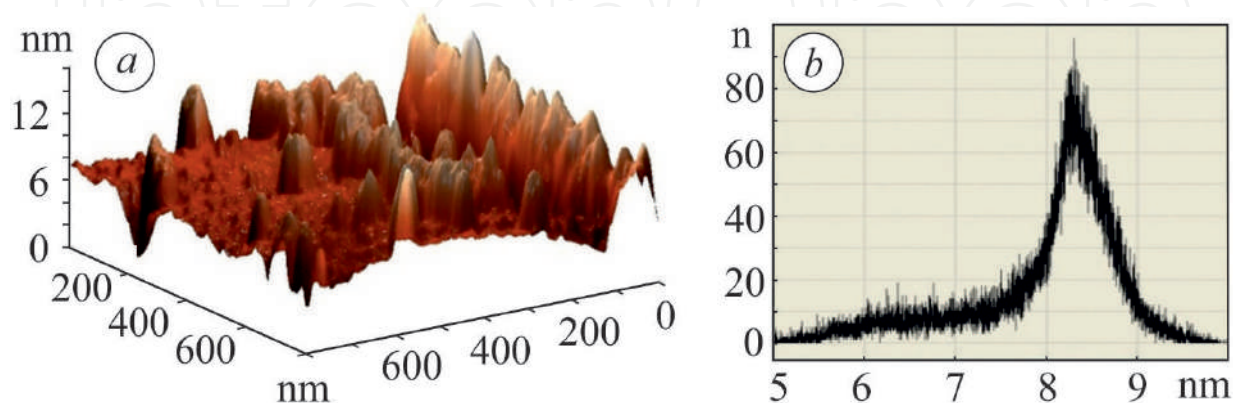


Figure 8. Character of distribution of synthesized Fe₃O₄-NP on the surface (a) and histogram of their distribution by size (b). Lateral dimension of particles in nanometers is given on X-axis, and a number of scanned particles on Y-axis.

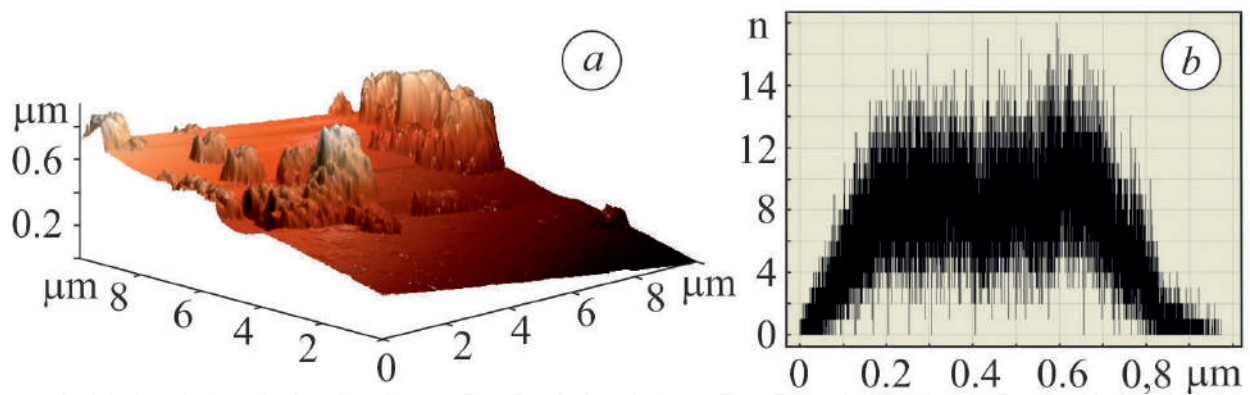


Figure 9. Character of distribution of synthesized microparticles of Fe_3O_4 (a) and histogram of their distribution by size (b). Transverse dimension of particles in nanometers is given on X-axis, and a number of scanned particles on Y-axis (b).

on the stress state, form and degree of ferromagnetic dispersion allows us to choose these physical parameters as the quality characteristics of phases. Just these factors that strongly affect the results of the quantitative X-ray analysis, in the magnetic phase analysis, practically have no effect on the investigation results.

To carry out magnetic phase analysis, it is necessary to build experimentally a temperature dependence of saturation magnetization of the tested material sample. Equipment for the analysis should provide measuring of magnetic properties in a wide range of temperatures and heating and cooling rates. Peculiarity of the determination of the transition temperature of a number of dispersive magnetic systems to the paramagnetic state is that their magnetic phase analysis must be performed at high heating rates. Since in a number of cases the mass of the investigated samples can be very small (nanomaterials, fine-dispersive powders, amorphous films, surface layers after different types of heat treatment) and as a result the value of the magnetic moment is relatively small (from 10^{-2} to $10^{-3} \text{ A}\cdot\text{m}^2$), the equipment must possess a very high sensitivity.

For such investigations, it is most reasonable to use the method of vibrating specimen that is realized through vibration magnetometers [26].

Measurement accuracy with vibration magnetometer depends on the calibration accuracy. We have proposed the method of comparison when magnetometer is calibrated using a standard with a known magnetic moment. As a standard, carbonyl iron of certain batches is used.

Application of the comparative method for calibration requires ensuring of the following conditions:

- insignificant changes in the position and deviation from the perfect sphere-like symmetry have no influence on a calibration constant;
- frequency and amplitude of vibrations remain constant;
- sample holder (container) introduces only an insignificant value to the signal value and can be subtracted from it; and
- signal voltage—linear function of the magnetic moment of the sample.

Two measuring methods are used in vibration magnetometers—direct or compensation. The last one, in its turn, is of two types: the method of current shell and differential method. Compensation method allows avoiding the dependence of measuring results on the values of amplitude and frequency of vibrations. It is optimal to perform high-temperature measuring preliminary assuming the measures of stabilization of sample mechanical vibration. Constant amplitude and frequency of sample vibrations is a required condition of providing an adequate accuracy of measuring by the direct method.

The main cause of vibration amplitude instability is the changes in the moving parts of the magnetometer. Stability of measuring parameters is determined, in addition, by the stability of the alternating current generator which feeds the vibrator. Vibration amplitude stabilization was realized by providing a negative feedback of the generator.

Such a device for investigation of the magnetic properties possesses a number of unique characteristics. At room temperature, it is possible to build a hysteresis loop, partial hysteresis loops, initial curves of magnetization and demagnetization, and dependence of a magnetic moment on the sample orientation. At elevated temperatures, thermomagnetic measurements, high-temperature hysteresis measurements, and time dependences of magnetic moment at different temperatures can be carried out. Temperature measuring interval ranges from 80 to 1100 K at power 3.5 kWt. Magnetic measurement in this work was performed using a vibration magnetometer [15]. Curves of the investigated samples over magnetization were recorded in magnetic fields from -200 kA/m to +200 kA/m by measuring the dependence of the given magnetization I/I_{200} on the magnetic field strength H , I_{200} —magnetization at magnetic field strength 200 kA/m.

As one can see, curves of Fe₃O₄-NP sample remagnetization have a nonhysteresis form with a zero coercive force H_c and residual magnetization I_r (**Figure 10(a)**). Probably particles of Fe₃O₄ due to a high degree of dispersivity are in a superparamagnetic state—state that is typical of microscopic and nanoscopic particles of ferromagnetic materials. In this case, a magnetic moment of the like particle changes its orientation spontaneously and randomly or due to thermal fluctuations. When external magnetic field is absent, superparamagnetics

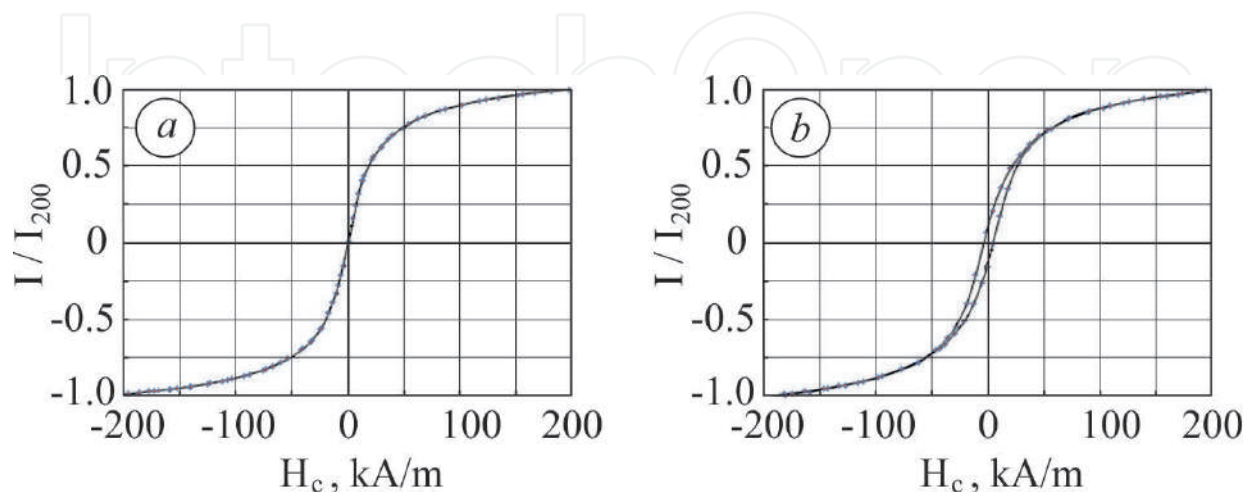


Figure 10. Curves of remagnetization of Fe₃O₄-NP (a) and Fe₃O₄-MP (b) samples.

have on average a zero magnetic moment, i.e., they behave like paramagnetics with a high magnetic susceptibility. As known, superparamagnetic properties of Fe_3O_4 particles at room temperature are exhibited, when reaching an average diameter $D < 25$ nm. In our case, the particles size is 5–10 nm.

With increasing sizes of Fe_3O_4 particles to microsized, the magnetic properties do not change. These particles have already a hysteresis loop (**Figure 10(b)**). Samples' coercive force is $H_c = 4$ kA/m, and ratio is $I/I_{200} = 0.1$.

2.5. Use of the Internet of Things to measure of magnetic properties

For a remote study of magnetic properties of nanoparticles, it is proposed in this work to use the approaches of the Internet of Things—a network that consists of the interrelated physical objects or devices that contain mounted gauges. Their software allows one to pass and exchange data between physical world and computer systems using the conventional procedure of communication. In addition to gauges, the network contains executing devices, built-in physical objects interrelated by wire or wireless nets. These interrelated objects possess function of reading, putting in operation, programming and identification of objects and also allow one to exclude the necessity of person participation due to application of the intellectual interfaces.

Technology of magnetic particle detection and characterization is based on many approaches of magnetic sensing techniques [27, 28].

Here we present novel 3D magnetic sensors which offer three-dimensional sensing of orthogonal B_x , B_y and B_z projections of magnetic field vector. Nowadays, many types of techniques and magnetic sensors provide such possibility [29, 30]. Among them, three types, namely magnetoresistors, Hall sensors and magnetotransistors, are preferable.

The first type, magnetoresistors, is based on the effect of magnetoresistance which is a tendency of material to change the value of its electrical resistance in an externally applied magnetic field. There are a variety of effects that can be called magnetoresistance: some occur in bulk nonmagnetic metals and semiconductors, such as geometrical magnetoresistance, Shubnikov de Haas oscillations, or the common positive magnetoresistance in metals. Other effects occur in magnetic metals, such as negative magnetoresistance in ferromagnets or anisotropic magnetoresistance (AMR). Finally, in multicomponent or multilayer systems (e.g., magnetic tunnel junctions), giant magnetoresistance, tunnel magnetoresistance and extraordinary magnetoresistance can be observed [31].

As an example, Honeywell International Inc. produced a series of magnetic sensors based on anisotropic magnetoresistance effect. AMR is a property of material in which the dependence of electrical resistance on the angle between the direction of electric current and the direction of magnetization is observed. AMR arises from the simultaneous action of magnetization and spin-orbit interaction, and its mechanism depends on the material. It can be for example due to a larger probability of s-d scattering of electrons in the direction of magnetization, which is controlled by the applied magnetic field.

AMR technology provides advantages over other magnetic sensor technologies. These anisotropic, directional sensors feature precision in-axis sensitivity, linearity, and low cross-axis sensitivity. For example, the HMC5883L is a small-size surface-mount, multi-chip module designed for low-field 3D magnetic sensing with a digital interface for applications such as low-cost compassing and magnetometry. The HMC5883L includes the state-of-the-art, high-resolution HMC118X series magnetoresistive sensors plus an application-specific integrated circuit, containing amplification, automatic degaussing strap drivers, offset cancellation and a 12-bit analog-to-digit converter.

The second type, Hall sensors, is based on Hall effect which is due to the nature of the current in a conductor. Current consists of the movement of many small charge carriers, typically electrons, holes or ions. When magnetic field is present, these charges experience a force, called the Lorentz force. When such a magnetic field is absent, the charges follow approximately straight “line of sight” paths between collisions with impurities, phonons and so on. However, when a magnetic field with a perpendicular component is applied, their paths between collisions are curved so that moving charges accumulate on one face of the material. This leaves equal and opposite charges exposed on the other face where there is a scarcity of mobile charges. The result is an asymmetric distribution of charge density across the Hall element, arising from the force that is perpendicular to both the “line of sight” path and the applied magnetic field. The separation of charge establishes an electric field that opposes the migration of further charge, so a steady electrical potential is established for as long as the charge is flowing.

We have proposed new type of thin-film magnetic field sensors for three-dimensional sensing of orthogonal B_x , B_y and B_z projection of magnetic field vector [32–37], new method for measuring magnetic field [38] as well as their modeling and signal processing [39–44].

The general view of such thin-film 3D sensors, its active area, structure and photographs are presented in **Figures 11–13**, correspondingly. The sensor (**Figure 12(a)**) active area is the thin sensitive semiconductor film (2) of corresponding configuration formed at the semi-insulating GaAs substrate (1). Sensor contacts are formed by the metallization layer (3), which typically is the gold film together with other metals, for example, with titanium sublayer. For manufacturing of the structures, three photolithographies are used. The first one is intended

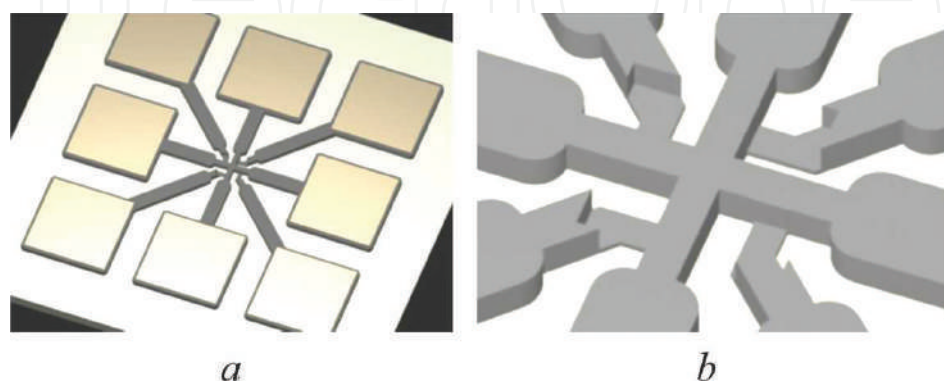


Figure 11. General view of thin film 3D sensors (a) and its active area (b).

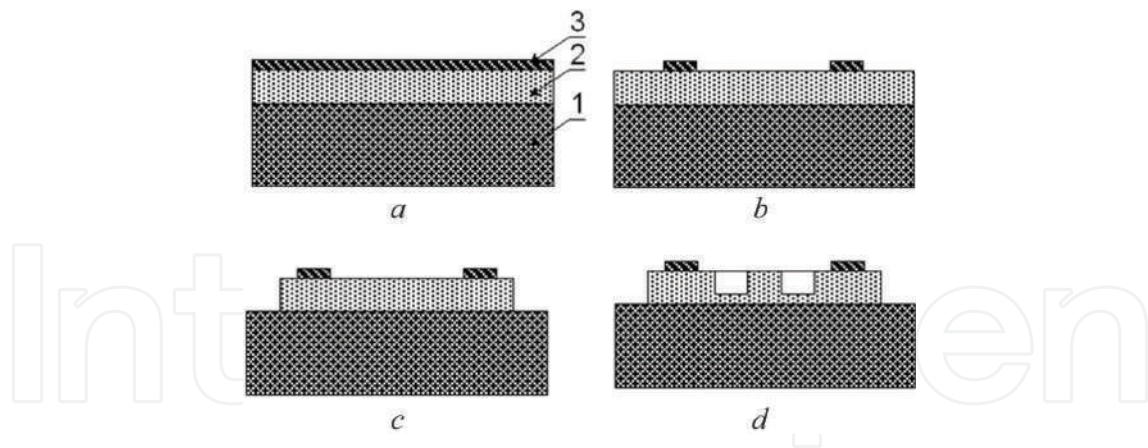


Figure 12. Structure and its formation stages (a), (b), (c), (d) of 3D thin film sensor: 1—substrate, 2—semiconductor active area; 3—contact metallization layer.

for creation of the contact system (**Figure 12(b)**); the second one is for etching a semiconductor film into the whole depth (**Figure 12(c)**); and the third one is for etching the semiconductor film to approximately 10% of their thickness (**Figure 12(d)**).

To show how a 3D thin-film sensor works, let us consider its main component—transducer #1 (**Figure 14**). The magnetic field vector projections B_x , B_y are located in the transducer plane, and B_z projection is perpendicular to this plane.

The operation principle of transducer of type #1 is the following: transducer is connected to the power source, typically direct current source; for this, the central current contact 3 is connected to the first power supply output, and side current outputs 4, 5 are connected together to the second power supply output. Thus, the current in the active area of the transducer is divided equally and run in mutually antithetical directions in relation to the current output.

Neglecting the current in the 6 and 7 voltage contacts' circuit, one may consider that the voltages at those outputs are equal to the corresponding voltages of the intermediate areas 10 and

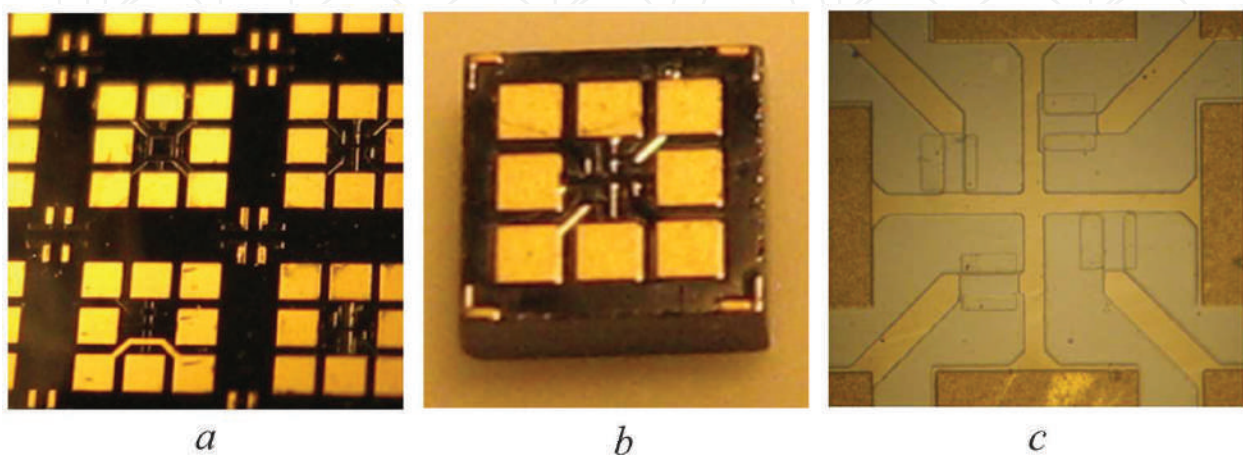


Figure 13. Photos of 3D thin-film sensors: wafer (a), chip (b) and active area (c).

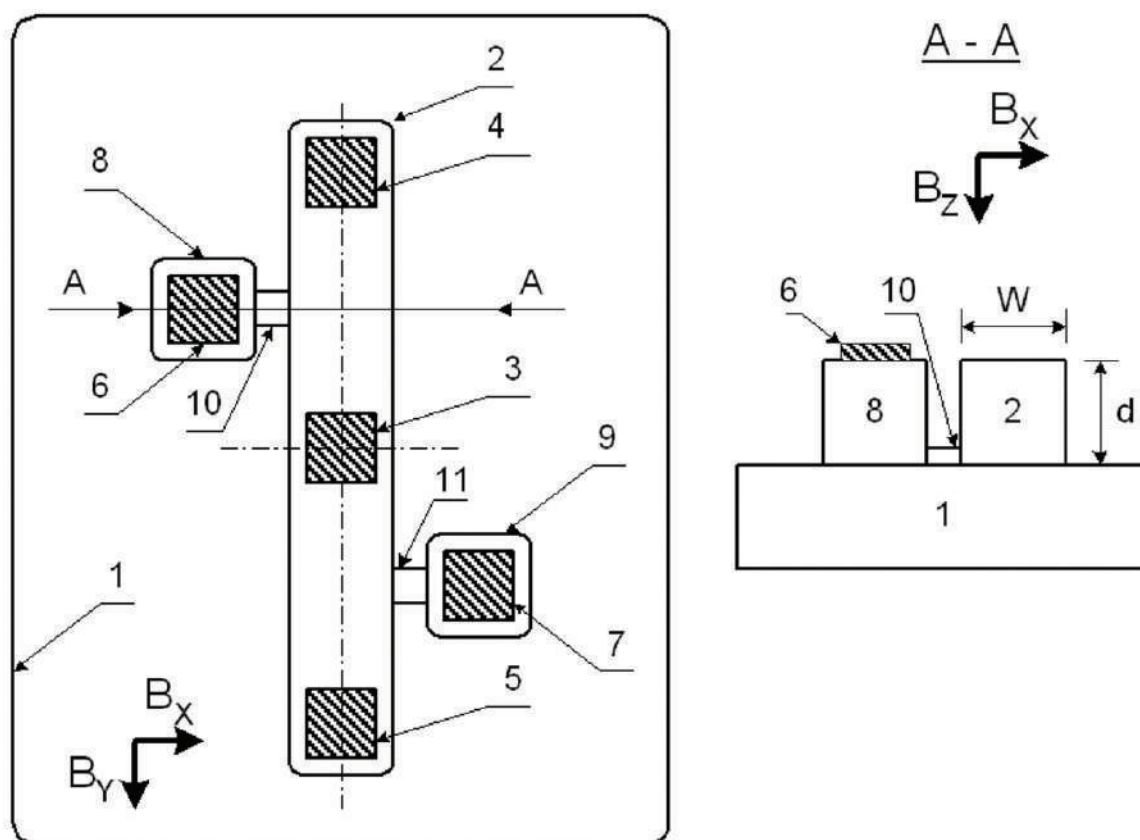


Figure 14. Structure of type #1 transducer: 1—substrate, 2—semiconductor active area; 3—central current contact; 4, 5—side current contacts; 6, 7—voltage contacts; 8, 9—auxiliary areas; 10, 11—intermediate areas.

11. So the construction of the type #1 transducer provides the possibility of forming the output voltage at the 6 and 7 voltage contacts, which is equal to the voltage difference between the areas of lower surface of the active area in the neighborhood for the contacting to the intermediate areas 10 and 11. The voltage measurement at the areas of lower active area surface is obvious that the thickness of intermediate areas 10, 11 was considerably thinner (at least 10 times) than the thickness of active area 2.

The principal difference of the type #1 transducer from analogs, for example Refs. [29, 30], is that in the first one the voltage difference is measured between the areas of lower active area surface, and in the analogs—between the areas of the upper active area surface. In its turn, the absence of contacts with the upper active area surface makes it possible not to perform the active area surface insulation.

In general case, the voltages at the voltage outputs 6, 7 are composed of three components. The first component V_R is caused by the voltage drop at the semiconductor active area 2. Taking into consideration the symmetry of the active area in relation to the first current contact 3, the first voltage component at both voltage contacts 6, 7 is equal $V_R(6) = V_R(7)$. The second component V_Z is caused by the influence of B_Z magnetic field vector projection, which is perpendicular to the transducer plane. Taking into consideration the transducer construction and current flow directions in it, the second voltage component at the voltage contacts 6 and 7 is also equal $V_Z(6) = V_Z(7)$. The third component V_X is caused by the influence of B_X projection

of induction vector. Contrary to the two stated above, this component at the voltage contacts 6 and 7 has the opposite signs $V_x(6) = -V_x(7)$. In particular, in the upper part of active area, two charge carriers under the influence of electromotive force deviated to the upper semiconductor layer surface, and then, in the lower part—to the lower surface (in the direction of substrate). The voltage difference caused by this carrier deviation is transferred to the voltage contacts 6 and 7 through the intermediate areas 10 and 11. It is to be noted that the B_y magnetic field induction vector projection, parallel to the direction of current flow through the active area, does not cause the carrier deviation, and therefore, it may be neglected: $V_y(6) = V_y(7) = 0$.

Thus, the voltage difference between the voltage outputs 6 and 7 (output voltage of type#1 transducer) is determined only by B_x magnetic field induction vector projection, and in first approximation, it does not depend on other vector projections:

$$V_{OUT} = [V_R(6) + V_x(6) + V_y(6) + V_z(6)] - [V_R(7) + V_x(7) + V_y(7) + V_z(7)] = V_x \quad (1)$$

where $V_x = V_x(6) + V_x(7)$.

The especially high efficiency of transducer of type#1 application is realized in case of their application in 3D sensor for simultaneous measurement of three projections B_x , B_y and B_z of the magnetic field induction vector. Such 3D sensor contains three coupled transducers at a single substrate. The construction of two transducers of #1 type is similar to **Figure 14**. They are mutually orthogonally rotated and provide the sensitivity to the B_x , B_y vector projections of the field induction vector. The third transducer, which provides the sensitivity to the B_z projection, is a traditional Hall transducer [29].

To provide the equal sensitivity levels for all three transducers of such 3D sensor, it is necessary to take into account the following: contrary to the traditional Hall transducers, which have the sensitivity as an inverse function of semiconductor active layer thickness d , the sensitivity of the transducer of type #1 is inversely proportional function of the semiconductor area width W . So it is recommended that the active area width W should be minimal and approximately equal to the semiconductor layer thickness d .

There are two other options to build up 3D magnetic thin film sensors. They are based on type #2 and type #3 transducers.

The structure of type #2 transducer is shown in **Figure 15**.

The type #2 transducer is fed by the direct current source, and one pair of mutually opposed current contacts (e.g., 3 and 5) is connected to one output of the power source (e.g., positive), and another pair (4 and 6 correspondently) to the other power source contact (negative, correspondently). In accordance with this connection scheme, the four current flow circuits are formed: I_{34} , I_{36} , I_{54} and I_{56} , where the indices in the marked currents correspond to the numbers of current contacts. These current flow circuits geometrically form the square sides. The matter of principal importance is that the currents that flow in opposed square sides are equal by value and opposed by sign: $\vec{I}_{34} = -\vec{I}_{54}$; $\vec{I}_{36} = -\vec{I}_{56}$. The output signal of transducer is the voltage difference between the voltage contacts. The informative signals about the magnetic field vector projections B_x , B_y , B_z are the voltages V_x , V_y , V_z , which in first approximation are determined as:

$$V_x = V_8 - V_{10}; V_y = V_7 - V_9; V_z = \{(V_8 - V_9) + (V_{10} - V_7)\} / 2 \quad (2)$$

The difference of type #2 transducer from its analog [29, 30] is the limitation of the area of current transition between the 2nd outer and 11 inner insulating areas. This provides the increase of the sensor sensitivity to the B_x, B_y magnetic fields and decreases the cross-impact between the informative signals.

The sensitivity increase is explained by the reduction of the transducer active area size. Contrary to the traditional Hall transducers (sensitive to the field B_z perpendicular to the transducer plane), where the size that determines the sensitivity is the active area thickness, in case of the B_x, B_y field transducers, the determinative size is the current scattering region. The smaller area occupies the current scattering region, the higher is the voltage difference between the two corresponding voltage contacts, and therefore the higher sensitivity is.

The structure of type #3 transducer is shown in **Figure 16**.

Arms 2, 4 and contacts 6, 8, 10, 12 form the first vertical Hall transducer, and arms 3, 5 and contacts 7, 9, 11, 13—the second vertical Hall transducer. The first transducer is intended for measuring the B_x magnetic field vector projection, and the second one—for measurement of B_y projection. The measurement principle of Hall transducers consists in forming the voltage difference at the voltage outputs during the deviation of charge carriers in the semiconductor area under the electromotive force influence.

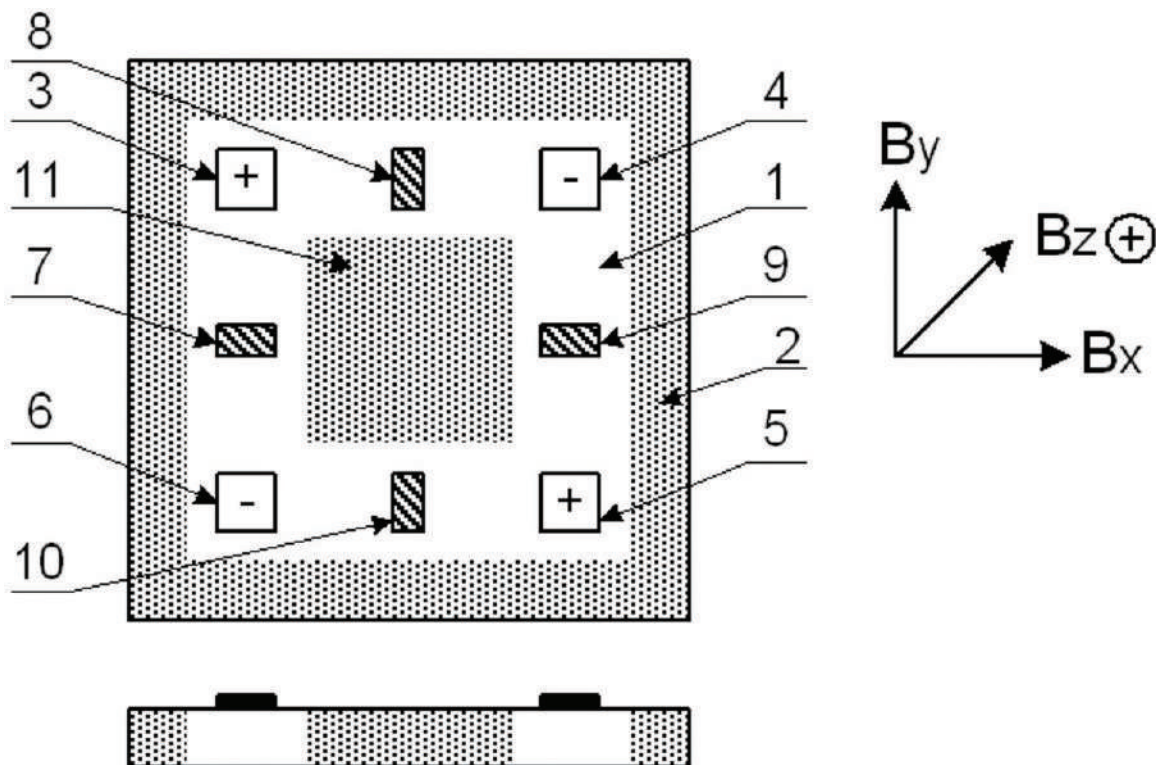


Figure 15. Structure of type #2 transducer: 1—semiconductor active area; 2—outer insulating area; 3, 4, 5, 6—current contacts; 7, 8, 9, 10—voltage contacts; and 11—inner insulating area.

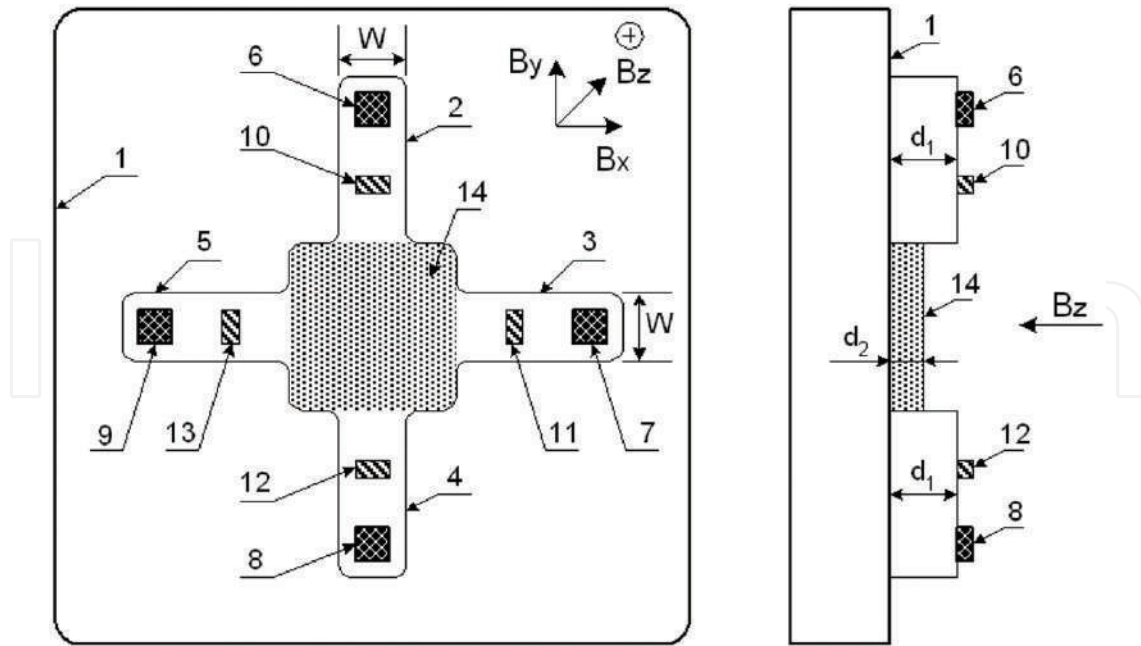


Figure 16. Structure of type #3 transducer: 1—substrate; 2, 3, 4, 5—four arms of cross-shaped figure, formed by the crossing of two semiconductor areas of vertical Hall transducers; 6, 7, 8, 9—current contacts; 10, 11, 12, 13—voltage contacts; and 14—semiconductor area of horizontal Hall transducer.

The operation of type #3 transducer presumes two power supplying modes. The first one provides the operation of the vertical Hall transducers, and the second one for operation of the horizontal one.

The first power-supplying mode presumes the connecting of the current contacts of the vertical Hall transducers, when the currents in their semiconductor areas are flowing in mutually opposed directions. For this, the current contacts of both vertical Hall transducers are connected into one circuit. Namely, contacts 6 and 8 of the first vertical Hall transducer are connected together and to the first, for example, positive output of the power source, and contacts 7 and 9 of the second vertical Hall transducer are also connected together to the second, therefore, negative output of the power source. So, in the first vertical Hall transducer, the currents are flowing from the top to the bottom (current I_2 in arm 2) and from the bottom to the top (current I_4 in arm 4), and in the second—from left to right (current I_3 in arm 3) and from right to left (current I_5 in arm 5). In case of ideal symmetry of the transducer structure, the following equality takes place: $\vec{I} = -\vec{I}; \vec{I} = -\vec{I}$.

Output signals of vertical Hall transducers are formed at the voltage outputs as a voltage difference, which is proportional to the multiplication of the power supply current value of the transducer by the corresponding magnetic field vector projection:

$$V_x = V(12) - V(10) = K_x \times I \times B_x / W \text{—for the first transducer and} \quad (3)$$

and

$$V_x = V(12) - V(10) = K_x \times I \times B_x / W \text{—for the second transducer and} \quad (4)$$

where $V(11)$, $V(12)$, $V(13)$ and $V(14)$ are the voltages at the voltage outputs 11, 12, 13 and 14, correspondingly; V_x , V_y and K_x and K_y —output signals and transducing coefficients of the first and second transducers, correspondingly; I —operational current, W —the width of semiconductor areas.

From the physical point of view, the appearance of voltage difference at the voltage contacts of the vertical Hall transducers is explained by the fact that due to the opposed current flow directions in both transducer arms, the deviation of current carriers in those arms has also the opposed direction. In particular, in arm 2 of the first transducer, the carriers are deviated in the direction away from the substrate to the surface of the semiconductor area, and then, in arm 4 of this transducer—in the direction from the surface to the substrate.

In a high-gradient magnetic field, the voltage difference formed at the voltage outputs of the vertical Hall transducers is the informative value of the averaged field induction value. Taking into the consideration that all the voltage outputs of the vertical Hall transducers are equidistant from its center (crossing area), the measured averaged induction value corresponds to the spatial point of the transducer center.

The second power-supplying mode presumes the application of only one pair of current contacts, namely 6 and 8 of the first vertical transducer. Then, output 6 is connected to the first power supply output, and output 8 to the second one. This provides the linear trajectory of the charge carriers in semiconductor area 14 of the horizontal Hall transducer.

The output signal of the horizontal Hall transducer, as a voltage difference, is proportional to the multiplication of the transducer power supply current by the B_z projection of the magnetic field induction vector, formed at the voltage outputs 11 and 13 of the second vertical Hall transducer: $V_z = V(13) - V(11) = K_z \cdot I \cdot B_z / d_2$, where K_z is the coefficient of transduction and d_2 is the thickness of semiconductor area of the horizontal Hall transducer.

From the physical point of view, the appearance of the voltage difference at the voltage outputs 11 and 13 is explained by the fact that charge carrier deviation in semiconductor area 14 of the horizontal Hall transducer under the influence of B_z magnetic field induction vector projection is in the direction from arm 5 to arm 3, or backwards.

As in the vertical transducer, the horizontal Hall transducer measures the value of the magnetic field induction value in the transducer center spatial point. Thus, type #3 transducer allows measuring of all three projections B_x , B_y and B_z of the magnetic field induction vector in a single spatial point.

The other distinctive feature of the type #3 transducer is the possibility to change the d_2 thickness of the horizontal Hall transducer semiconductor area. This allows the formation of the transducer with equal sensitivity value to all three magnetic field induction vector projections: $V_x/B_x = V_y/B_y = V_z/B_z$. Taking into consideration that the sensitivity of vertical Hall transducers is inversely proportional to the semiconductor area width W , and for horizontal transducer—to the thickness of its semiconductor area d_2 , the equality of the stated values of sensitivity is provided by the correspondent selection of W/d_2 ratio. It is important that contrary to the d_1 thickness of the vertical Hall transducer areas, the d_2 thickness of the horizontal transducer semiconductor area may change after the output formation. In particular, the decrease of d_2 thickness may be realized by partial etching of the semiconductor layer.

In relation to the analogs [29], the type #3 transducer provides the increase of the measurement accuracy and construction simplification.

The increasing accuracy is caused by the fact that horizontal Hall transducer is placed in the center (crossing area) of vertical Hall transducer. This provides the high spatial alignment of all transducers (two vertical and one horizontal), and therefore, all the three projections B_x , B_y and B_z of the magnetic field induction vector are measured at a single spatial point. During the measurement of high-gradient fields, this gives the ability to decrease the magnetic field induction vector measurement error in several times.

The third type, magnetoresistors, is mostly bipolar or field-effect transistors whose structures and operating conditions are optimized with respect to the magnetic sensitivity of its output currents. There are three major effects of magnetotransistors, namely the current deflection effect, the injection modulation and the magnetodiode effect.

We have proposed the structure of magnetotransistors adapted to three dimensional sensing of orthogonal B_x , B_y and B_z projections of the magnetic field vector (**Figures 17–19**). These are drift-aided lateral double-collector p-n-p transistors. The emitter area E and two collector p-type areas $C1$, $C2$ are embedded into plate-like n-type base region. The two base contact n⁺ type areas $B1$, $B2$ are used to apply the bias voltage needed to establish the lateral accelerating electric field in the region. The emitter injects holes into the base region. Under the influence of the accelerating field in the base, these holes form a minority carrier beam. In the presence of normal B_z magnetic field (**Figure 17**), the electric field in the base region rotates for the Hall angle of majority carries, and the hole beam tilts with respect to the electric field for the Hall

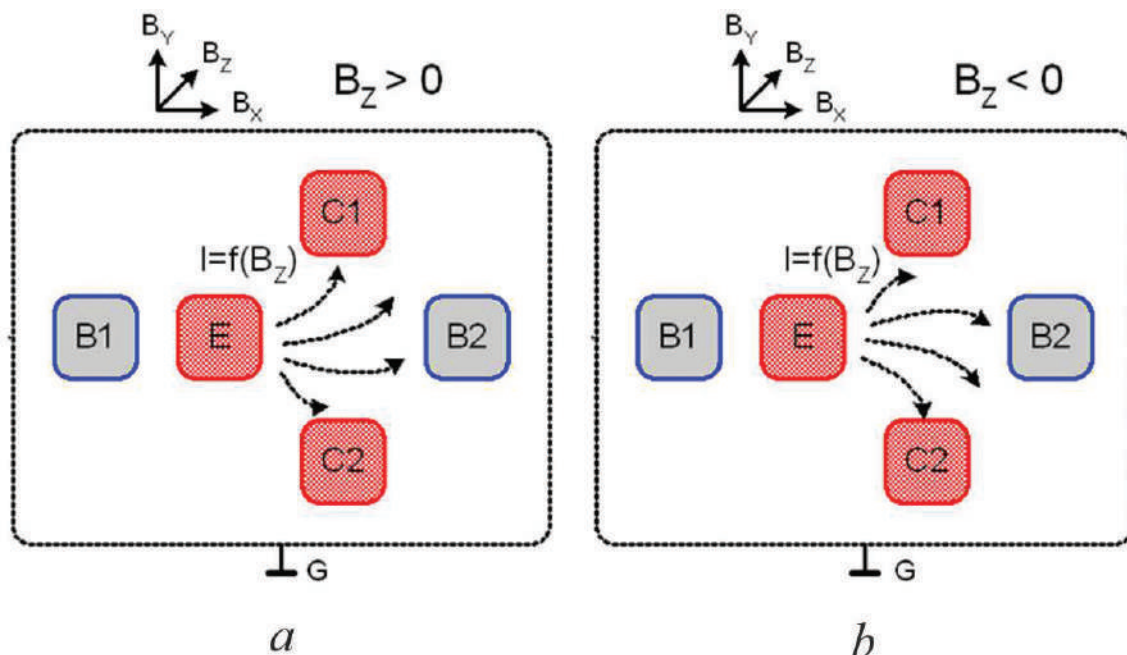


Figure 17. Structure of magnetotransistor (a) and current deflection (b) $I = f(B_z)$ under B_z magnetic field vector projection: $B1$, $B2$ —base contacts; E —emitter area; $C1$, $C2$ —collector areas; and G —connected to ground a p-n junction wall insulation.

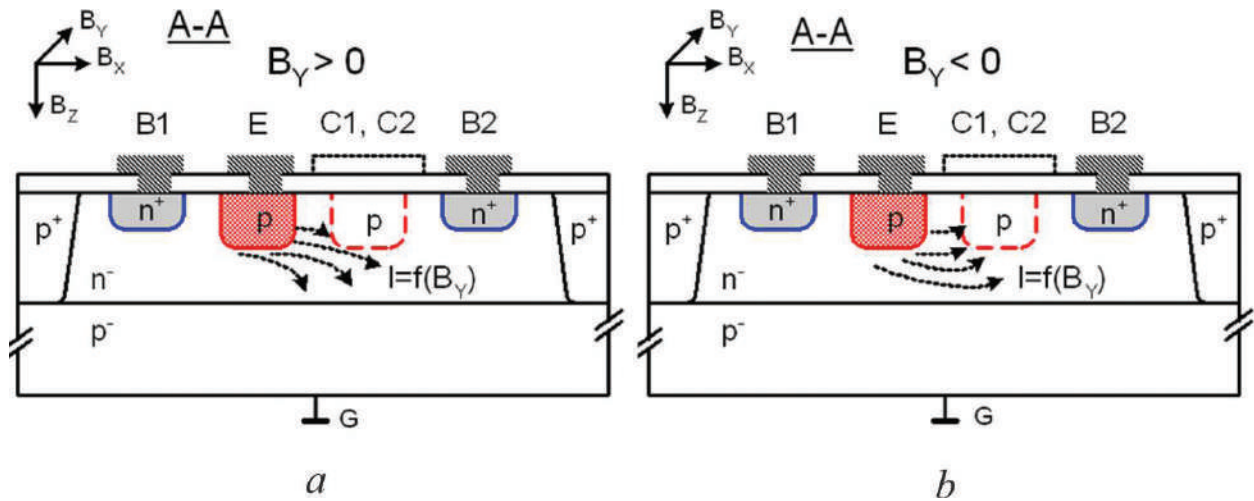


Figure 18. Structure of magnetotransistor (a) and current deflection (b) $I = f(B_Y)$ under B_Z magnetic field vector projection: B1, B2 (n^+ type)—base contacts; E (p type)—emitter area; C1, C2 (p type)—collector areas; G—a substrate connected to ground (p^- type).

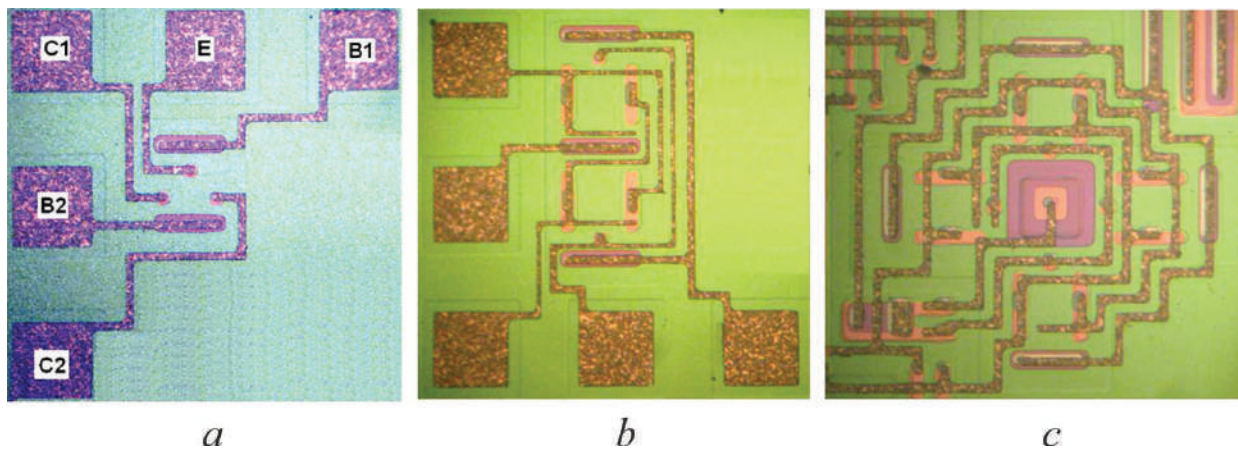


Figure 19. Photos of magnetotransistors: single (a), doubled (b) and quad (c) structures.

angle. The deflection of a beam leads to an imbalance in the two C1, C2 collector currents. In the presence of B_Y magnetic field vector projection (**Figure 18**), the hole beam tilts up to collectors or down toward a p^- type substrate connected to ground. Doubled and quad (**Figure 19**) structures are used to provide a set of signals in correspondence with three projections of magnetic field vector.

Based on the sensors proposed and described above, a set of magnetometers for detection and characterization of magnetic particles has been developed. For illustration only, an example of software windows for control and measurement result visualization, as well as a measurement resolution archived (in this case about 10^{-7} T), are shown in **Figures 20** and **21**. As it was noted, the main advantage of such sensors is a possibility of measuring three orthogonal projections of a magnetic field vector that is quite new in characterization of magnetic particle technique.

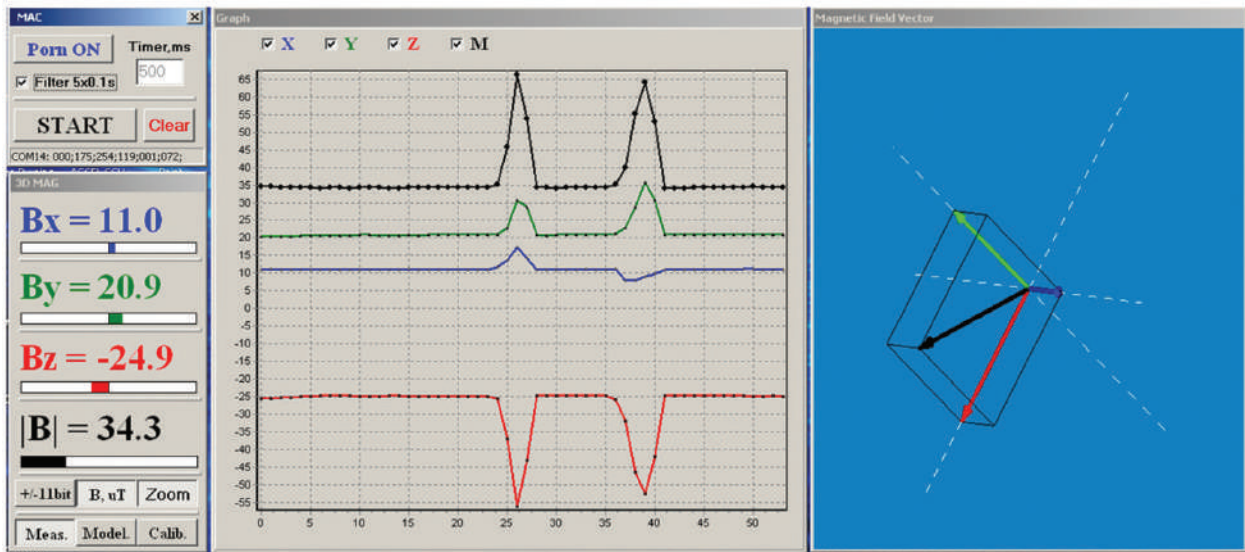


Figure 20. Software of magnetometer based on 3D sensors.

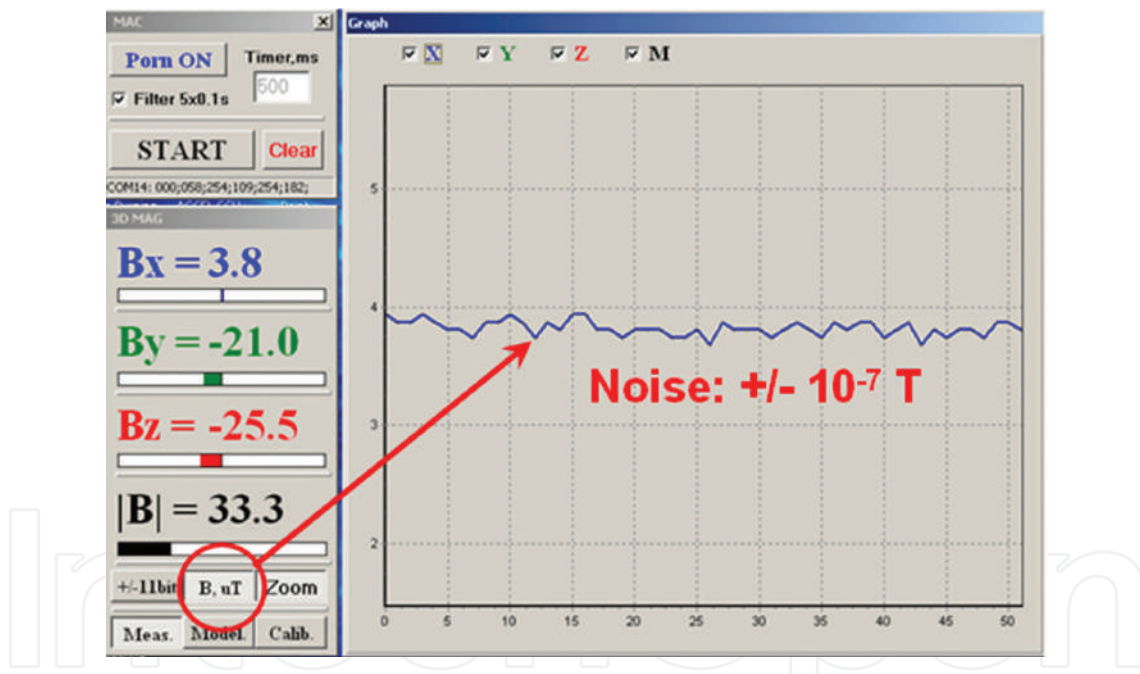


Figure 21. Measurement resolution (noise) of magnetometer based on 3D sensors.

3. Conclusion

It is possible to say that the interest to nanomaterials with magnetic properties increases every year. These materials have found their applications in medicine for diagnostics and treatment of serious diseases, where treatment by other methods is more expensive and durable. However, synthesis of such nanomaterials with stable properties is not completely elaborated, since besides the size factor, the character of their building microgeometry, functional

properties and methods of identification should be considered. Special attention should be paid to sizes, topography and biocompatibility of initial nanoparticles. Just these parameters finally determine the functional properties.

It is shown in the paper that identification of synthesized nanoparticles can be realized most effectively by the change of their magnetic properties. This is possible both at the stage of their synthesis and after biofunctionalization. Success of the proposed approach formed the basis of the ideology of the Internet of Things use for monitoring the stability of nanoparticles microstructure and their functional properties in application in medicine.

Acknowledgements

We are infinitely grateful to Mykhailo Gonchar and Tetiana Prokopiv from the Institute of Cell Biology of the National Academy of Sciences of Ukraine, Department of Analytical Biotechnology, for kindly provided samples of Fe₃O₄ powders for our research. Also we would like to acknowledge financial support of the Ministry of Education and Science of Ukraine under Grant 0116U004142 and partially by funds of 543994-TEMPUS-1-2013-1-BE-TEMPUS-JPCR MMATENG (Modernization of two cycles (MA, BA) of competence-based curricula in Material Engineering according to the best experience of Bologna Process – EU).

Author details

Zoia Duriagina^{1*}, Roman Holyaka¹, Tetiana Tepla¹, Volodymyr Kulyk¹, Peter Arras² and Elena Eyngorn³

*Address all correspondence to: zduriagina@ukr.net

1 Lviv Polytechnic National University, Lviv, Ukraine

2 KU Leuven, Sint-Katelijne-Waver, Belgium

3 Technische Universität Berlin, Berlin, Germany

References

- [1] De Crozals G, Bonnet R, Farre C, Chaix C. Nanoparticles with multiple properties for biomedical applications: A strategic guide. *Nano Today*. 2016;**11**(4):435-463
- [2] Nikiforov VN. Biomedical applications of magnetic nanoparticles. *Nauka i tehnologii v promyishlennosti*. 2011;**1**:90-99
- [3] Filippousi M, Angelakeris M, Katsikini M, Paloura EC, Efthimiopoulos I, Wang Y, Zamboulis D, Van Tendeloo G. Surfactant effects on the structural and on the magnetic properties of iron oxide nanoparticles. *Journal of Physical Chemistry C*. 2014;**118**(29):16209-16217. DOI: 10.1021/jp5037266

- [4] Uvarova IV, Maksymenko VB. Bio-compatible Materials for Medical Products. Kyiv: KiM; 2013. p. 232
- [5] Fang C, Zhang M. Multifunctional magnetic nanoparticles for medical imaging applications. *Journal of Materials Chemistry*. 2009;**19**:6258-6266. DOI: 10.1039/B902182E
- [6] Peng S, Wang C, Xie J, Sun S. Synthesis and stabilization of monodisperse Fe nanoparticles. *Journal of the American Chemical Society*. 2006;**28**:10676-10677
- [7] Gillich T, Acikgöz C, Isa L, Schlüter AD, Spencer ND, Textor M. PEG-stabilized core-shell nanoparticles: Impact of linear versus dendritic polymer shell architecture on colloidal properties and the reversibility of temperature-induced aggregation. *ACS Nano*. 2013;**7**:316-329
- [8] Lalatonne Y, Paris C, Serfaty JM, Weinmann P, Lecouvey M, Motte L. Bis-phosphonates-ultra small superparamagnetic iron oxide nanoparticles: A platform towards diagnosis and therapy. *Chemical Communications*. 2008;**22**:2553-2555
- [9] Hosseini AG, Bagheri M, Mohammad-Rezaei R. Synthesis and fluorescence studies of dual-responsive nanoparticles based on amphiphilic azobenzene-contained poly(monomethyl itaconate). *Journal of Polymer Research*. 2016;**23**(8):12. DOI: 10.1007/s10965-016-1061-y
- [10] Rozenfel'd LH, Chekman IS, Tertyshna AI. Nanotechnology in medicine, pharmacy and pharmacology. *Farmakolohiya ta likars'ka toksykolohiya*. 2008;**1-3**:3-14
- [11] Barrera C, Herrera AP, Bezares N, Fachini E, Olayo-Valles R, Hinestroza JP, Rinaldi C. Effect of poly(ethylene oxide)-silane graft molecular weight on the colloidal properties of iron oxide nanoparticles for biomedical applications. *Journal of Colloid and Interface Science*. 2012;**377**:40-50
- [12] Liu Y, Li Y, Li XM, He T. Kinetics of (3-aminopropyl)triethoxysilane (APTES) silanization of superparamagnetic iron oxide nanoparticle. *Langmuir*. 2013;**29**:15275-15282
- [13] Sun J, Zhou S, Hou P, Yang Y, Weng J, Li X, Li M. Synthesis and characterization of biocompatible Fe₃O₄ nanoparticles. *Journal of Biomedical Materials Research Part A*. 2006;**80**(2):333-341
- [14] Shu Z, Wang S. Synthesis and characterization of magnetic nanosized Fe₃O₄/MnO₂ composite particles. *Journal of Nanomaterials*. 2009;**2009**:340217. DOI: 10.1155/2009/340217
- [15] Ahangaran F, Hassanzadeh A, Nouri S. Surface modification of Fe₃O₄/SiO₂ microsphere by silane coupling agent. *International Nano Letters*. 2013;**3**:23
- [16] Arsalani N, Fattahi H, Nazarpour M. Synthesis and characterization of PVP-functionalized superparamagnetic Fe₃O₄ nanoparticles as an MRI contrast agent. *EXPRESS Polymer Letters*. 2010;**4**(6):329-338
- [17] Husain Q. Magnetic nanoparticles as a tool for the immobilization/stabilization of hydrolases and their applications: An overview. *Biointerface Research in Applied Chemistry*. 2016;**6**(6):1585-1606
- [18] Huang HY, Lovell JF. Advanced functional nanomaterials for theranostics. *Advanced Functional Materials*. 2017;**27**(2):1603524. DOI: 10.1002/adfm.201603524

- [19] Pankhurst Q, Connolly J. Applications of magnetic nanoparticles in biomedicine. *Journal of Physics D: Applied Physics*. 2003;**36**:167-181
- [20] Xu C, Sun S. New forms of superparamagnetic nanoparticles for biomedical applications. *Advanced Drug Delivery Reviews*. 2013;**65**:732-743
- [21] Long NV, Thi CM, Yong Y, Cao Y, Wu H, Nogami M. Synthesis and characterization of Fe-based metal and oxide based nanoparticles: Discoveries and research highlights of potential applications in biology and medicine. *Recent Patents on Nanotechnology*. 2014;**8**:52-61
- [22] Huang DJ, Lin H-J, Okamoto J, Chao KS, Jeng H-T, Guo GY, Hsu C-H, Huang C-M, Ling DC, Wu WB, Yang CS, Chen CT. Charge-orbital ordering and Verwey transition in magnetite measured by resonant soft X-ray scattering. *Physical Review Letters*. 2006;**96**(9):096401. DOI: 10.1103/PhysRevLett.96.096401
- [23] Radisavljevic I, Kuzmanovic B, Novakovic N, Mahnke HE, Vulicevic LJ, Kurko S, Ivanovic N. Structural stability and local electronic properties of some EC synthesized magnetite nanopowders. *Journal of Alloys and Compounds*. 2017;**697**:409-416. DOI: 10.1016/j.jallcom.2016.11.090
- [24] Nikiforov VN, Ignatenko AN, Irhin VY. The magnetism of the magnetite nanoparticles: Effects of finite size and coating. *Izvestiya RAN. Seriya fizicheskaya*. 2014;**78**(10):1336-1340. DOI: 10.7868/S0367676514100159
- [25] Duriagina ZA, Holyaka RL, Borysyuk AK. Automated widely diapazon magnetometer for magnetic alloys phase analysis: Development and application. *Uspehi Fiziki Metallov*; 2013;**14**:33-66
- [26] Kondyr AI, Borysyuk AK, Pazdriy IP, Shvachko SH. The use of a vibrating magnetometer for phase analysis of special steels and alloys. *Vybratsyy v tekhnike y tekhnologiyakh*. 2004;**34**(2):41
- [27] Koh I, Josephson L. Magnetic nanoparticle sensors. *Sensors*. 2009;**9**:8130-8145. DOI: 10.3390/s91008130
- [28] Janssen XJA, van Ijzendoorn LJ, Prins MWJ. On-chip manipulation and detection of magnetic particles for functional biosensors. *Biosensors and Bioelectronics*. 2008;**23**:833-838. DOI: 10.1016/j.bios.2007.08.023
- [29] Popovic RS. Hall Effect Devices. CAT# IPE331. 2nd ed. Bristol and Philadelphia, USA; CRC Press, 2003. p. 420. ISBN: 9780750308557. Available from: <https://www.crcpress.com/Hall-Effect-Devices-Second-Edition/Popovic/p/book/9780750308557>
- [30] Popovic DR, Dimitrijevic S, Blagojevic M, Kejik P, Schurig E, Popovic RS. Three-axis teslameter with integrated Hall probe. *IEEE Transactions on Instrumentations and Measurement*. 2007;**56**(4):1396-1402. DOI: 10.1109/TIM.2007.900133
- [31] wikipedia.org. Magnetoresistance [Internet]. Available from: <https://en.wikipedia.org/wiki/Magnetoresistance>
- [32] honeywell.com. 3-Axis Digital Compass IC HMC5883L [Internet]. 2010. Available from: https://aerocontent.honeywell.com/aero/common/documents/myaerospacecatalog-documents/Defense_Brochures-documents/HMC5843.pdf

- [33] Bolshakova I, Holyaka R. Multiposition 3-D Magnetic Field Sensor [Internet]. European Patent Office, Patent No. WO2005029604. 2005. Available from: https://worldwide.espacenet.com/searchResults?ST=singleline&locale=en_EP&submitted=true&DB=&query=WO2005029604
- [34] Bolshakova I, Holyaka R. Method for Measuring Magnetic Field [Internet]. European Patent Office, Patent No. WO2012054000. 2012. Available from: https://worldwide.espacenet.com/searchResults?ST=singleline&locale=en_EP&submitted=true&DB=&query=WO2012054000
- [35] Bolshakova I, Holyaka R. Magnetic Field Measuring Sensor [Internet]. European Patent Office, Patent No. WO2006028425. 2006. Available from: https://worldwide.espacenet.com/searchResults?ST=singleline&locale=en_EP&submitted=true&DB=&query=WO2006028425
- [36] Bolshakova I, Holyaka R. Magnetic Field Measuring Sensor [Internet]. European Patent Office, Patent No. WO2006028427. 2006. Available from: https://worldwide.espacenet.com/searchResults?ST=singleline&locale=en_EP&submitted=true&DB=&query=WO2006028427
- [37] Bolshakova I, Holyaka R. Magnetic Field Measuring Sensor [Internet]. European Patent Office, Patent No. WO2006028426. 2006. Available from: https://worldwide.espacenet.com/searchResults?ST=singleline&locale=en_EP&submitted=true&DB=&query=WO2006028426
- [38] Bolshakova I, Holyaka R, Murari A. Method for Measuring Magnetic Field [Internet]. European Patent Office, Patent No. EP2630511. 2015. Available from: https://worldwide.espacenet.com/searchResults?ST=singleline&locale=en_EP&submitted=true&DB=&query=EP2630511
- [39] Bolshakova I, Holyaka R, Gerasimov S. Magnetic Field Measurement with Continuous Calibration [Internet]. European Patent Office, Patent No. GB2427700. 2009. Available from: https://worldwide.espacenet.com/searchResults?ST=singleline&locale=en_EP&submitted=true&DB=&query=GB2427700
- [40] Hotra Z, Holyaka R, Marusenkova T, Ilkanych V. Algorithms of semiconductor magnetic field sensor devices power consumption minimization. In: ELNANO; 2012; Kyiv. pp. 29-30. Available from: http://journals.kpi.ua/publications/text/29_30_2012.pdf
- [41] Hotra Z, Holyaka R, Marusenkova T. Optimization of microelectronic magnetic sensors on the splitted Hall structures. In: Prace Instytutu Elektrotechniki, editor. Proceedings of Electrotechnical Institute, Instytut Elektrotechniki. Issue 247. 2010. pp. 13-18. Available from: <https://pbn.nauka.gov.pl/polindex-webapp/browse/article/article-4d222aa0-9679-45e1-9467-5c5de8b262f6>
- [42] Hotra Z, Holyaka R, Bolshakova I, Yurchak I, Marusenkova T. Spatial models of splitted Hall structures. In: Proceedings of VIIth International Conference on Perspective Technologies and Methods in MEMS Design; MEMSTECH-2011; IEEE.2011. pp. 5-8. Available from: <http://ieeexplore.ieee.org/document/5960249/>

- [43] Holyaka R, Yurchak I, Marusenkova T, Ilkanych V. Microprocessor noise-immune signal transducer for galvanomagnetic smart sensor devices. In: International Conference on Modern Problems of Radio Engineering Telecommunications and Computer Science; TCSET-2012; IEEE.2012. p. 430. Available from: <http://ieeexplore.ieee.org/document/6192682/>
- [44] Bolshakova I, Holyaka R, Hotra Z, Marusenkova T. Methods of modeling and calibrating 3D magnetic sensors based on splitted Hall structures. Electronics and Nanotechnologies. Proceedings of the XXXI International Scientific Conference. 2011; p. 38. Available from: http://www.journals.kpi.ua/publications/text/2011_38.pdf

IntechOpen

